# Photoelectrochemical advanced oxidation processes for removal of azo dye from water: emerging aspects and oxidation products

**Abdulgalim Isaev** ( abdul-77@yandex.ru )
Dagestan State University: Dagestanskij gosudarstvennyj universitet https://orcid.org/0000-0002-1659-0661
**Nabi Shabanov**
Dagestan State University: Dagestanskij gosudarstvennyj universitet
**Murtazali Rabadanov**
Dagestan State University: Dagestanskij gosudarstvennyj universitet
**Zhu Mingshan**
Jinan University

**Research Article**

**Keywords:** Photoelectrochemical, advanced oxidation processes, azo dye, removal, wastewater, photoelec-trocatalytic, photoelectro-Fenton, solar photoelectro-Fenton

**Posted Date:** May 16th, 2023

**DOI:** https://doi.org/10.21203/rs.3.rs-2808914/v1

# Photoelectrochemical advanced oxidation processes for removal of azo dye from water: emerging aspects and oxidation products

Abdulgalim Isaev [1]*, Nabi Shabanov [1,2], Murtazali Rabadanov[1], Zhu Mingshan[3]

[1]Department of Inorganic Chemistry and Chemical Ecology, Dagestan State University, st. M. Gadjieva 43-a, Dagestan Republic, 367015 Makhachkala, Russia; abdul-77@yandex.ru

[2]Dagestan Federal Research Centre of the Russian Academy of Sciences, Analytical Center for Collective Use, Gadzhiyev str. 45, 367000, Makhachkala, Russia

[3]Guangdong Key Laboratory of Environmental Pollution and Health, School of Environment, Jinan University, Guangzhou, 511443, PR China

*Correspondence: abdul-77@yandex.ru Tel.: +79634279778

## Abstract

Azo dyes are one of the large classes of water soluble synthetic dyes with a wide range of colors and can be released into the environment when used. Azo dyes belong to one of the most numerous groups of synthetic dyes and are characterized by the presence of an azo group (-N=N-) with two or more symmetrical or asymmetrical aromatic radicals. Processes of photoelectrochemical oxidation using various approaches have been developed for the removal of azo dyes from wastewater. The fundamentals of different photoelectrochemical oxidation processes for azo dyes, such as photoelectrocatalytic oxidation (PEC), photoelectro-Fenton (PEF), and solar photoelectro-Fenton (SPEF) processes, are discussed. The use of different semiconductor materials as electrode materials in photoelectrocatalysis and PEF for azo dye removal, the influence of different parameters on the removal of azo dyes from wastewater, reactor design, combined photoelectrochemical oxidation, including the use of fuel cells, are also considered. The anodic, electrochemical, and photoelectrochemical oxidation processes for azo dye removal is compared. Also shows what products are mainly formed during photoelectrochemical oxidation of azo dyes and how photoelectrochemical oxidation affects the toxicity of azo dye solutions under different conditions.

Key words: Photoelectrochemical, advanced oxidation processes, azo dye, removal, wastewater, photoelectrocatalytic, photoelectro-Fenton, solar photoelectro-Fenton.

## 1. Introduction

The color of wastewater is one of the regulated parameters for discharge into the environment. The presence of organic dyes gives wastewater an increased coloration (Bilińska and Gmurek 2021). Synthetic dyes are characteristic of wastewater from their production and from technological processes of dyeing various materials, particularly in textile industry, dry cleaning, etc. (Castillo-Cabrera et al. 2022). The textile indus-try is the most water-intensive and consumes a large amount of water resources. Therefore, the creation of closed-loop water supply systems for the textile industry is one of the acute problems.

Synthetic dyes contained in wastewater from the textile industry are biologically resistant compounds and pose a threat to natural ecosystems and humans due to their potential bio-toxicity. Therefore, a large number of technologies are being developed and implemented for re-moving synthetic dyes from wastewater, including chemical, electrochemical, photochemical, and photo-electrochemical technologies (de Queiroz et al. 2017; Ganiyu et al. 2018). Advanced oxidation processes (AOP) have great potential, and compared to other methods (e.g., coagulation and adsorption) has high efficiency for removing synthetic dyes and does not cause secondary pollution (Ma et al. 2021). AOP is considered an environmentally safe method since organic dyes can be completely mineralized by oxidation with hydroxyl radicals (•OH). The high standard oxidation-reduction potential ($E°$=2.80 V (vs. NHE)) of the hydroxyl radical provides its ability to oxidize most organic pollutants (Nidheesh et al. 2018; Brillas 2020). Recently, electrochemical oxidation processes have attracted attention because they allow for continuous and on-site generation of oxidants under mild conditions, which avoids the addition of various chemicals for dye oxidation (Oturan 2014; Mousset and Dionysiou 2020; Ganiyu et al. 2021; García-Espinoza et al. 2021). Electrochemically generated oxidants, particularly •OH, is complete mineralization of organic dyes (Brillas and Martínez-Huitle 2015). Electrochemical methods include heterogeneous processes such as anodic oxidation and photoelectrocatalysis, in which •OH is formed on the surface of the anode either electrochemically or photochemically, and homogeneous processes such as electro-Fenton, photo-electro-Fenton, and sono-electrolysis, in which •OH is formed mainly in the solution (Sirés et al. 2014a; Brillas 2020) . In recent years, photoelectrocatalytic oxidation methods have been intensively developed for dye removal because their use increases the efficiency of oxidation due to the synergistic effect of combined photochemical reactions and electrolysis reactions (Laghrib et al. 2021). The photoelectrocatalytic removal of synthetic dyes has certain advantages compared to photocatalysis and electrocatalysis. The main advantages include high charge separation efficiency compared to photocatalytic dye removal and low energy consumption compared to electrocatalytic dye removal. In addition, thin film semiconductor electrodes are used

for the process of photoelectrocatalytic oxidation of azo dyes, which solves the problem of separation the catalyst from purified water. The use of solar energy to carry out the photoelectrocatalytic process with use the high-sensitivity photocatalysts to sunlight is also an obvious advantage (Zhang et al. 2023).

The use of photoelectrocatalytic technologies allows for the removal of hard oxidation organic dyes from wastewater (Ochiai and Fujishima 2012). The main electrode material used for photoelectrocatalytic dye removal is titanium dioxide ($TiO_2$). Over the past years, a wide variety of $TiO_2$-based materials have been investigated as it is the most stable, inexpensive, accessible, and effective material for dye oxidation (Karanasios et al.; Of et al. 2009; Ge et al. 2016). The photoelectrocatalytic characteristics of other semiconductor materials, such as ZnO, $SnO_2$, $WO_3$, $Fe_2O_3$, CdS, and BiOX (X = Cl, Br, I), have also been inten-sively studied for creating dye removal technology using solar energy (visible light) (Zhang et al. 2009; Peleyeju and Arotiba 2018; Orudzhev et al. 2020; Ahmed et al. 2020; Rajput et al. 2021; Castillo-Cabrera et al. 2022).

The rapid recombination of photo-generated electrons/holes ($e^-/h^+$) is the main disadvantage of using photocatalytic processes (Daghrir et al. 2012; Divyapriya et al. 2021; Yusuf et al. 2022). Applying an external potential to the photocatalyst reduces charge recombination (Brillas 2020). The combination of electrochemical and photo-catalytic technologies allows for the separation of photo-generated electrons and holes, prevent-ing their recombination (Ye et al. 2021). The use of photoelectrocatalytic processes increases the efficiency of removing synthetic dyes from wastewater and reduces energy costs when using solar energy (Zhang et al. 2012; Shabanov et al. 2017; Chen et al. 2022b). Therefore, the photoelectrocatalytic method is currently considered one of the most promising methods for removing organic compounds from wastewater. The use of such hybrid processes increases the efficiency of the process due to a synergistic effect (Yuan et al. 2021).

This article provides a review of studies dedicated to the photoelectrocatalytic oxidation of azo dyes, one of the largest classes of synthetic dyes. The widespread use of azo dyes is due to their ease of application, diverse properties, wide range of colors from yellow to black, high lightfastness, and use in various industries such as textile, paint, and printing for coloring differ-ent products. Azo dyes can color most types of natural, artificial, and synthetic fibers, including leather, plastic, rubber, and more. Most azo dyes are soluble in water, coloring of different materials and therefore generate a large amount of wastewater (Bafana et al. 2011). The focus is on the use of photoelectro-catalysis, photoelectro-Fenton, and solar photoe-lectro-Fenton processes for removing azo dyes. Particular attention is paid to materials and heterostructures as photoelectrocatalysts with high efficiency in the use of light and the separation of photogenerated charges, which increases their redox characteristics and leads to higher rates of neutralization of azo dyes.

The toxicity of azo dye solutions and their inter-mediates after treatment are briefly discussed to understand issues related to preventing water pollution using the latest developments in photoelectrocatalytic removal of various classes of azo dyes.

## 2. Theoretical aspects of photoelectrocatalysis

The photocatalysis process was first used for water decomposition using $TiO_2$ as a photocatalyst (Fujishima and Honda 1972). For photocatalytic water decomposition, a minimum bandgap energy of 1.23 eV is required, which corresponds to the redox potentials of $H^+/H_2$ and $O_2/H_2O$ pairs (Lu et al. 2016). However, to ensure electron transfer and subsequent hydrogen evolution reactions, a larger bandgap (> 2.0 eV) is often required. At the same time, the photocatalyst should have a small enough bandgap for efficient use of solar energy (Eg <3.0 eV) (Qu and Duan 2013). Compared to photocatalytic processes using powdered photocatalysts, photoelectrocatalytic processes promote the separation of electrons and holes (Ma et al. 2020).

When semiconductors are irradiated with UV or sunlight, n-type material is used as a photoanode, and it generates electron vacancies, which release oxygen (Equation 1). The generated electrons move to the photocathode, where hydrogen evolution reaction occurs (Equation 2) (Fig. 1a).

$$2H_2O + 4h^+ \rightarrow O_2 + 4H^+,\ E^0_{O_2/H_2O} = 1{,}23\ V \text{ vs. } RHE \qquad (1)$$

$$2H^+ + 2e^- \rightarrow H_2,\ E^0_{H^+/H_2} = 0\ V \text{ vs. } RHE \qquad (2)$$

The oxygen evolution reaction has thermodynamic limitations, where the minimum conduction band of the semiconductor should be more negative than the energy level of $H^+/H_2$, while the maximum valence band should be more positive than the energy level of $O_2/H_2O$ (Qu and Duan 2013).

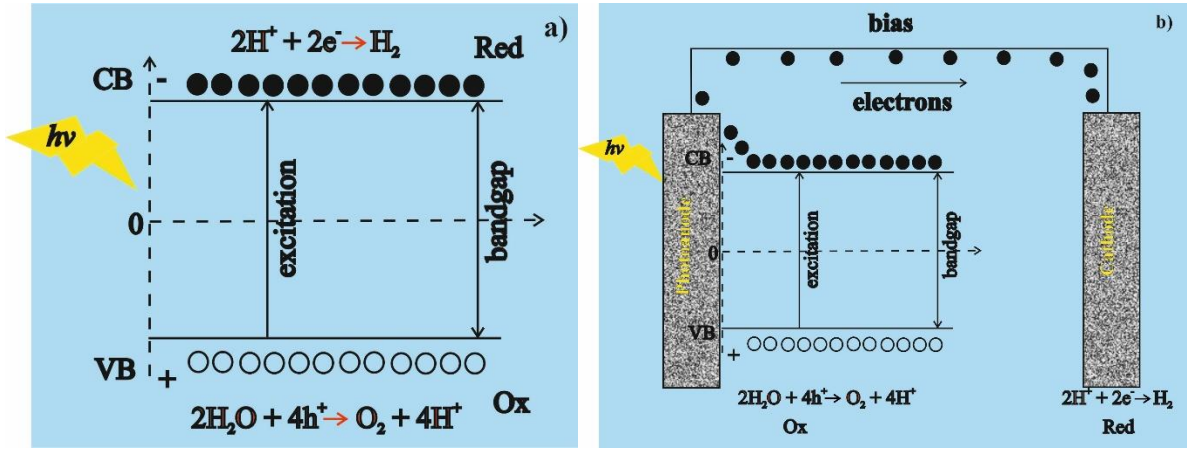


Fig. 1. a – Scheme of electron and hole pair generation on semiconductors by irradiation UV or sunlight; b – Photoelectrochemical separation of charges with the formation of electrons and holes.

For photoelectrocatalytic oxidation of organic compounds, photocathodes made of semiconductors deposited to various substrates and capable of reacting to UV or solar light are used, which are irradiated with light with energy equal to or greater than the bandgap with simultaneous application of external potential (Cao et al. 2017; Kusmierek 2020). Absorption of a quantum of light by the semiconductor photocathode with energy greater than its bandgap results in the separation of charges with the formation of electrons ($e^-$) in the conduction band and holes in the valence band (Fig. 2b) (Rajput et al. 2021). Under the influence of an externally applied potential, photo-generated $e^-$ can be moved to the counter electrode, leading to redox reactions on the electrode surfaces (Cao et al. 2017). Simultaneously with the electrolysis process, direct oxidation reactions of azo dyes and the formation of highly active oxygencontaining particles occur on the photocatalyst surface (Feng et al. 2021). The combination of electrocatalytic and photocatalytic processes decrease the rate of electron-hole pair recombination and increasing hole lifetime. However, photo-generated electrons and holes can also recombine and release heat, reducing quantum efficiency (Zarei and Ojani 2016).

In order for a photocatalytic process to proceed on a semiconductor electrode, it must be irradiated with energy greater than its bandgap energy, leading to the generation of a pair of $e^-/h^+$ (Garcia-Segura and Brillas 2017):

$$MetO + h\nu \rightarrow e^- + h^+ \quad (3)$$

The generated holes act as oxidizers, while electrons act as reducers. The resulting h+ has strong oxidizing ability and can migrate to the surface for direct interaction with organic substances or interact with $H_2O/OH^-$ to form hydroxyl radicals, which also oxidize organic pollu-tants. Photogenerated electrons can react with dissolved oxygen to form active oxygencontaining particles according to reaction (5) (Garcia-Segura and Brillas 2017).

$$h^+ + H_2O \rightarrow {}^{\bullet}OH + H^+ \quad (4)$$

$$e^- + O_2 \rightarrow O_2^{\bullet -} \quad (5)$$

Other oxygencontaining particles, such as hydroperoxyl radical $HO_2^{\bullet}$ and hydrogen peroxide, can be formed during reactions (6) and (7):

$$O_2^{\bullet -} + H^+ \rightarrow HO_2^{\bullet} \quad (6)$$

$$2\,HO_2^{\bullet} \rightarrow H_2O_2 + O_2 \quad (7)$$

The electrons and holes generated by the photocatalytic process are unstable and can to return to their base state or through reaction with adsorbed •OH according (6) or predominantly through recombination with unreacted $h^+$ (7) (Bessegato et al. 2015; Meng et al. 2015).

$$e^- + {}^{\bullet}OH \rightarrow OH^- \quad (8)$$

$$e^- + h^+ \rightarrow \text{catalyst} + \text{heat} \quad (9)$$

In addition to photocatalytic processes on the metal oxide semiconductors, electrochemical oxidation of organic compounds can also occur. Anodic oxidation of organics can occur through direct electron transfer to the anode surface and hydroxyl radicals formed on the anode surface during water oxidation. The efficiency of hydroxyl radical formation and, consequently, the oxidation of azo dyes depends on the anode material. Since the process of forming •OH is a heterogeneous process, the use of active metallic and metal oxide anodes leads to chemisorption of products of azo dye oxidation on the electrode surface and their low activity in oxidation process (Panizza and Cerisola 2009). Anodes with high oxygen evolution overpotential, such as boron-doped diamond (BDD), $PbO_2$, and others, contribute to the formation of hydroxyl radicals (Peralta-Hernández et al. 2012; Alimirzaeva et al. 2019; He et al. 2019; Karim et al. 2021). This is due to the oxidation of water to an adsorbed hy-droxyl radical Met(•OH):

$$MetO + H_2O \rightarrow M(^{\bullet}OH) + H^+ + e^- \quad (10)$$

The low conductivity of the oxide semiconductor materials used in the photoelectrocatalytic process allows only small values of anodic current density to be applied (no more than 10 $mA/cm^2$), which is characterized by a low rate of hydroxyl radical formation. The use of high anodic potentials leads to a loss of photocatalyst characteristics (Garcia-Segura and Brillas 2017).

## 3. Photoelectrocatalytic oxidation

The efficiency of photoelectrocatalytic oxidation of azo dyes depends on the type of background electrolyte, pH, electrode potential, semiconductor electrode material and type of irradiation source used, as well as the initial concentration of the pollutant, photoanode surface morphology, and reactor design. $TiO_2$, $WO_3$, $SnO_2$, ZnO, CdS, BDD, etc. are mainly used as electrode materials in the photoelectrocatalytic oxidation of azo dyes (Hepel and Hazelton 2005; Isaev et al. 2012; Orudzhev et al. 2019).

In the photoelectrocatalytic oxidation of azo dyes on metal oxide electrodes, first of all, the nitrogen-nitrogen bond (-N=N-) breaks, which leads to discoloration of the solution (Subba Rao et al. 2017). When comparing electrocatalytic and photoelectrocatalytic oxidation of azo dyes, the efficiency for the photoelectrocatalysis process is much higher. For example, when using $SnO_2$–$Sb_2O_4$ as an anode, a decrease in color up to 88% was achieved at 240 min of electrolysis, while in photoelectrolysis, the decrease in color was 93%. Deposition on $SnO_2$ -$Sb_2O_4$ of $WO_3$ resulted in an increase in both color and COD removal efficiency. It was found that the percentage of COD removal using the $SnO_2$-$Sb_2O_4$-$WO_3$ electrode is 78 and 84%, respectively, under the conditions of electrocatalysis and photoelectrocatalysis (Subba Rao et al. 2017).

$TiO_2$ obtained using various approaches, was used as a photoanode in the photoelectrocatalytic oxidation of azo dyes. Larbi K.H. et al. (Larbi et al. 2021) reported on $TiO_2$ films synthesized

from $TiCl_3$ on conductive glass substrates (ITO) using direct and pulsed electrodeposition for the oxidation of methyl orange (MO). Thin films of $TiO_2$ deposited on FTO-coated glass substrates using the method of sputtering onto a heated substrate were used for the photoelectrocatalytic oxidation of azo dyes in aqueous solutions of Active Red 152 (AR152) (Ali et al. 2018) and Acid Orange 7 (AO7) (Shinde et al. 2009). The efficiency of oxidation of AR152 was 70% when illuminated with ultraviolet light after 120 minutes of photoelectrocatalysis (Ali et al. 2018). The $TiO_2$ film obtained using the sol gel technology also exhibits good catalytic activity in the oxidation of a mixture of Reactive Orange 16 (orange), Reactive Black 5 (RB5) (black), and Reactive Red RB 133 (red) azo dyes (Cervantes et al. 2013).

The use of $TiO_2$ nanotubes obtained by electrochemical anodization for the oxidation of various azo dyes has great interes. During the oxidation of azo dyes Disperse Red 1, Disperse Red 13, and Disperse Orange 1 on Ti/$TiO_2$ nanotubes, the decrease in total organic carbon (TOC) was ≥87% after 240 minutes of treatment (Ferraz et al. 2013). Arrays of $TiO_2$ nanotubes have a larger specific surface area than a film of $TiO_2$ particles, which leads to an increase in their adsorption capacity and charge transfer rate (Qiu et al. 2018). An increase in the rate of MO oxidation on arrays of $TiO_2$ nanotubes compared to a TiO2 film obtained by the sol-gel technology was observed Zhao Q. et al. (Zhao et al. 2009). At the same time, the use of $TiO_2$ obtained by plasma electrolytic oxidation leads to an increase in the efficiency of oxidation of the azo dye Drimaren Red 243 X6BNB compared to $TiO_2$ obtained by titanium anodization (Franz et al. 2015).

Various approaches are used to increase the efficiency of photoelectrocatalytic oxidation of azo dyes. In particular, to increase the efficiency of the oxidation of azo dyes by increasing the activity of $TiO_2$ due to doping with various metals and non-metals are used. The use as doping elements of metal atoms leads to the excitation of $TiO_2$ under visible light irradiation (Zhang et al. 2013). Boron-doped $TiO_2$ was used for photoelectrocatalytic oxidation of acid red 151 Acid Red 151 (AR151) in 0.01 mol/l $Na_2SO_4$ as an electrolyte. Complete discoloration of the solution was observed within 30 minutes, and complete mineralization was achieved after 90 min of photoelectrocatalysis (Bessegato et al. 2019). On tellurium-doped $TiO_2$, a complete decolorization of a solution of reactive yellow 105 was achieved within 60 minutes under visible light irradiation (Nurdin et al. 2022). For another azo dye, such as reactive orange 84 with an initial concentration of 0.5 ppm, a 98% discoloration of the solution was achieved within 60 min during photoelectrocatalytic oxidation on selenium-doped $TiO_2$/Ti under sunlight irradiation (Tian et al. 2021).

On lanthanum doped $TiO_2$ nanoparticles electrode the efficiency of photoelectrocatalytic oxidation of MO with a concentration of 15 mg/L under UV light irradiation was more than 90% at 140 minutes. At the same time, compared with pure $TiO_2$ nanoparticles, the efficiency of oxidation of azo dye on La doped $TiO_2$ was 26.17% higher (Xing et al. 2013). For the same dye,

copper-modified TiO2 showed a higher efficiency. There, 92.88% MO discoloration was achieved in a solution with a concentration of 0.5 ppm at 60 minutes when irradiated with visible light (Nurdin et al. 2021). A photoanode based on a $TiO_2$ film doped with Fe and fabricated by the sol-gel method, when UV light irradiated at 3 hours, showed a degree of discoloration of the MO solution of 85% (Tang et al. 2014).

$TiO_2$ based heterostructures show good efficiency of the oxidation of azo dyes. This can be explained by the synergistic effect associated with the formation of a p-n-heterojunction between a p-type and n-type semiconductors, which increases the photogenerated electron transfer rate, which improving the photocatalytic properties of semiconductors and a decrease of the photogenerated electron-hole pairs recombination rate due to voltage application during photoelectrolysis (Isaev et al. 2022). Photoelectrocatalytic oxidation of X-3B azo dye (CI Reactive red 2) (X-3B) using the cerium doped $TiO_2$ nanoparticles deposited on a film of BDD showed that the degradation rate during photoelectrocatalysis was higher than the sum of photocatalysis and electrooxidation processes (Wang et al. 2011). The same effect was also demonstrated for an electrode made of a graphene-$TiO_2$ (D-P25) composite film prepared by dipping. The percentage degradation of X-3B during photoelectrolysis on a D-P25 sample containing 1% graphene after 25 minutes of the process increased from 36.4% to 71.8% with increasing applied potential from 0 to 2.0. V (relative to saturated Ag/AgCl), and for samples containing 2 and 3% graphene - 41.6–78.7% and 38.3–73.8%, respectively (Wang et al. 2012). The oxidation efficiency of Acid Red 33 (AR33) azo dye on a titanium electrode coated of multi-walled carbon nanotubes and titanium dioxide composite (MWNT–$TiO_2$/Ti) was 98% solution discoloration and 41.66% mineralization after 60 min of treatment at a current density of 7.5 mA cm–2 and pH = 5.2 (Nabizadeh Chianeh and Basiri Parsa 2015).

Photoelectrocatalytic oxidation of MO using $TiO_2$ nanotube (NT) heterostructures was demonstrated in works (Deng et al. 2018; Zeng et al. 2021). The results of the studies showed that heterostructures exhibit higher activity during electrocatalysis (EC), photocatalysis (PC), and photoelectrocatalysis (PEC) than the initial $TiO_2$ NTs. Comparison of the electrocatalytic, photocatalytic and photoelectrocatalyticprocesses of azo dyes oxidation for all heterostructures showed that the efficiency of oxidation increases in the range: EC<PC<PEC. For example, when MO oxidation on $TiO_2$ NTs under optimal conditions showed 16.1% mineralization with EC, 39.4% with PC, and 78.0% with PEC at 60 min under irradiation of a 350 W xenon lamp. Under the same conditions, the mineralization efficiency of MO on $CeO_2$/$TiO_2$ NT is 23.2%, 56.5%, and 98.1%, respectively, which is mainly due to good absorption of visible light and a higher efficiency of charge carrier separation (Fig. 2) (Deng et al. 2018).

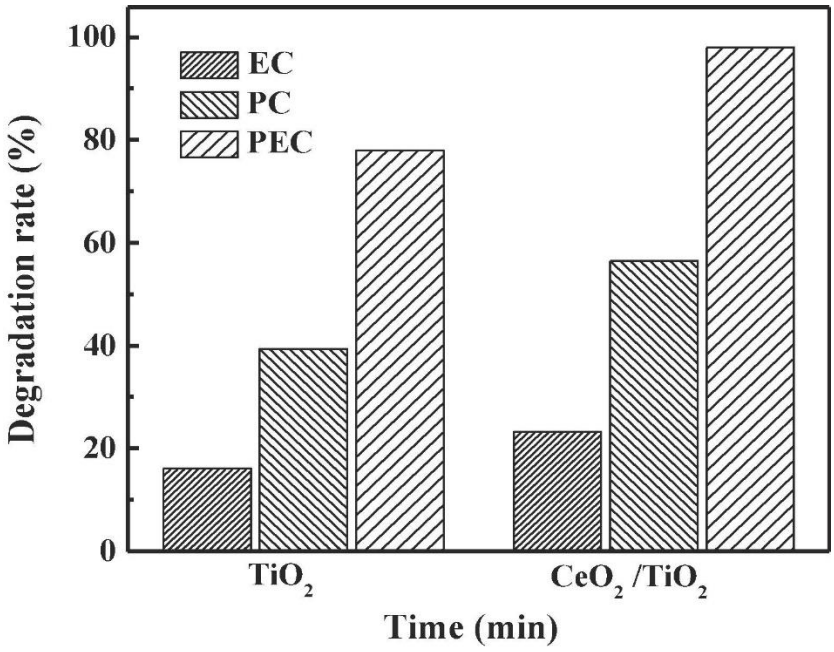


Fig. 2. Efficiency of MO degradation on $TiO_2$ NT and $CeO_2/TiO_2$ NT photoelectrodes under simulated solar irradiation. Reprinted by permission from (Deng et al. 2018). Copyright 2018, Elsevier.

The MO photoelectrocatalytic oxidation on a $ZnO/TiO_2$ electrode under UV light irradiation, complete removal of the dye was achieved after 90 min, while in the photocatalytic process at the same time only 39.6% MO removal was obtained (Zhang et al. 2008). Compared to the $TiO_2$ NT electrode, the efficiency of MO oxidation on $CdS/TiO_2$ NT increased from 78% to 99.2% under UV light at 2 h and from 14% to 99.2% at 3 h under visible light irradiation (Jiang et al. 2011). A higher MO oxidation rate is observed when using $TiO_2$–$SiO_2$ ceramic nanostructures formed by anodization of the Ti surface using sodium hexafluorosilicate electrolyte. Complete discoloration of MO 100% was observed after 70 min of photoelectrolysis (Mumjitha and Raj 2015). This is due with use of NaCl as an electrolyte and the generation of active chlorine, but, unfortunately, the authors did not indicate which light source was used for irradiation. Complete removal of another azo dye of AO7 by photoelectrocatalytic oxidation under optimal conditions and irradiation with visible light requires 180 min, and a complete reduction of COD is achieved after 270 min (Ghalebizade and Ayati 2016).

$WO_3$ based photoanodes have also been used for photoelectrocatalytic oxidation of azo dyes. Discoloration of the MO solution on $WO_3$ obtained by electrochemical anodization of tungsten foil was shown in (Zheng and Lee 2014). As $TiO_2$, the $WO_3$ is characterized by a higher efficiency in decolorization of an azo dye solution by photoelectrocatalysis than photocatalysis or electrocatalysis. On $WO_3$ based composite photoanodes, such as $W/WO_3/TiO_2$, the efficiency of TOC removal during the oxidation of azo dye basic red 51 using UV and visible light iraadiation

is 94 and 88%, respectively (Fraga et al. 2013). $WO_3/TiO_2$ heterostructures with layered structure, high crystallinity, a large specific surface area, and strong light absorption in the solar spectrum visible region, is show the high activity of the photoelectrocatalytic oxidation of active red 152 (Hunge et al. 2018). Kusmierek E. et al. (Kusmierek and Chrzescijanska 2015) conclude that it is possible to use the $WO_3$ modified $TiO_2$–$RuO_2$/Ti electrodes for the photoelectrocatalytic oxidation of azo dyes not only under UV irradiation, but also under visible light irradiation, for example, sunlight or room lighting lamps.

Heterostructures based on $Fe_2O_3$ were also used as electrode materials to the photoelectrocatalytic oxidation of azo dyes. For example, an α-$Fe_2O_3/TiO_2$/activated carbon (α-$Fe_2O_3$/TiO2/ACP) nanocomposite obtained by electrophoretic deposition was used as an electrode for decolorization of azo dye active yellow 39 under the visible light irradiations. The results showed that the decolorization efficiency the visible light photoelectrocatalytic process using the α-$Fe_2O_3/TiO_2$/ACP nanocomposite was higher (94%) compared to those for $TiO_2$/ACP (45%) and α-$Fe_2O_3$/ACP (60.26%) under optimal conditions (Ayoubi-Feiz et al. 2014). The $Fe_2O_3/TiO_2$ nanotube electrode exhibited a higher photoelectrocalytic activity to MO degradation in an acidic medium. At an initial pH 3, the rate of MO solution discoloration reach 91.7% under UV-light irradiation at 5 min (Cong et al. 2012). The thin-film $Sn_3O_4/TiO_2$/Ti electrode showed high efficiency the mono-azo dye Acid Yellow 17 (AY17) oxidation under visible light and achiev 95% color removal after 60 minutes at pH 2. At low potentials (0.5 V), the efficiency of photoelectrocatalytic color removal increased to 97.% and TOC removal 83% with rate almost 3 times higher than with photocatalysis (Huda et al. 2019). The use of the $TiO_2$ NT/$Bi_2MoO_6$ composite leads to complete discoloration of the MO solution under sunlight irradiation at 3 hours, which is mainly associated with the formation of a type II heterojunction between $TiO_2$ and $Bi_2MoO_6$ [76]. The type II heterojunction not only enhances the efficiency of visible light absorption, but also increase the transfer of photogenerated charge carriers and limits the recombination of electron–hole pairs by use of an internal electric field [59]. The same efficiency at the level of 95% at the oxidation of active green 19 under visible light irradiation is shown by the $TiO_2$/Ti electrode decorated with $FeTiO_3$ (Azis et al. 2021).

Other semiconductors and heterostructures based have been studied at the photoelectatalytic oxidation of azo dyes. The $YFeO_3$/Carbon fiber composite electrode provides high photoelectrocatalytic activity by the removal of RB5 with visible light irradiation and efficiency of 99% after a 60-minute treatment (Liu et al. 2021). The Orange II oxidation efficiency on bismuth ferrite (BFO) and 10% La-BFO photoanodes was 55.3% and 84.2%, respectively (Nkwachukwu et al. 2021). Electrodes $SnO_2$-$Sb_2O_4$-$WO_3$ during photoelectrolysis for 120 min showed complete discoloration of the trypan blue dye solution with 84% COD removal at the same time (Subba Rao

et al. 2017). The use of a Ti/Pt/$PbO_2$ electrode as a photoanode at the oxidation of direct red 80 (DR80) leads to increase the process efficiency compared to other electrode materials. Complete discoloration of the Direct Red 80 solution was achieved after 4 hours of treatment at an initial dye concentration of 25.0 mg/l and a current of 50 mA (Florêncio et al. 2013). A composite of exfoliated graphite and bismuth vanadate was used as a photoanode to the oxidation of AO7 and the dye removal efficiency was 88% at 90 minutes (Orimolade and Arotiba 2019). The high efficiency of photoelectrocatalytic oxidation of acid red 1 was achieved on the Ni@ZnO/$MoS_2$ composite. The presence of MoS2 improves the catalytic properties of the composite, which is mainly associated with the formation of p-n junctions between ZnO and $MoS_2$ (Fei et al. 2020).

The electrolyte type also affects the efficiency of the photoelectrocatalytic oxidation of azo dyes. A comparison of the photoelectrocatalytic oxidation of AO7 on nanocrystalline TiO2 films in NaCl and $Na_2SO_4$ solutions showed that the oxidation of the azo dye in NaCl solution occurs mainly due to the electrochemical generation of active chlorine (Tantis et al. 2015). The presence of ammonium persulfate ($(NH_4)_2S_2O_8$) in solution significantly increases the efficiency of removal due to the formation of $SO_4^{\bullet-}$ radicals, which was demonstrated in (Thabet and El-Zomrawy 2016) during the oxidation of the azo dye acid red 17. Non-radical $(NH_4)_2S_2O_8$ activation mechanism demonstrated at the use of the visible-light-sensitive ternary structure $TiO_2$-graphene oxide–phthalocyanine Zn nanosheets ($TiO_2$ @GONS@ZnPc) for the photoelectrochemical degradation of azo dye Orange G (Nwahara et al. 2021).

Another advantage of the photoelectrocatalytic process is the use of carbon-based cathode materials for the generation of hydrogen peroxide due to the cathodic reduction of oxygen, which leads to an increase in the efficiency of the photoelectrocatalytic process (Ghalebizade and Ayati 2016). An increase in the aeration rate leads to an increase the solubility of oxygen with a corresponding increase to the yield of hydrogen peroxide [89, 90]. To increase the yield of hydrogen peroxide during the photo-electrochemical oxidation of the direct black dye 22 are shown in works (Isaev et al. 2013; Isaev et al. 2018), photoelectrolysis is carried out at elevated oxygen pressures of 0.1 to 0.7 MPa.

Table 1 shows the comparative characteristics of various materials used as photoanodes at the oxidation of azo dyes.

357 Table 1. Comparative characteristics of various materials used as photoanodes at the photoelectrocatalytic oxidation of azo dyes

| Photoanode | Synthesis method | Azo dye | Process parameters | Light source | Discoloration | Ref |
|---|---|---|---|---|---|---|
| $TiO_2$–$RuO_2$/Ti electrodes modified with $WO_3$ | thermal decomposition | Acid Orange 7 | 0.1 mol/l $Na_2SO_4$<br>$[Dye]_0$ = 200mg/l<br>2h at 0.01 $Acm^2$ | UV and Vis irradiation | 98.63 | (Kusmierek and Chrzescijanska 2015) |
| Fe-doped $TiO_2$ | sol–gel method. | Methyl orange | 2 V<br>$[Dye]_0$ = 10 mg/L<br>3 h | 300 W Xenon arc lamp | 85% | (Tang et al. 2014) |
| $Cu^{2+}$-doped $TiO_2$ | sol–gel method, using dip-coating as the coating way | Methyl orange | 1 h<br>1.0 V | two UV lamps (?max = 365 nm, 8 W | | (Zhang et al. 2013) |
| $TiO_2$ NT | anodization | Methyl orange | 0.1 M $Na_2SO_4$<br>light intensity = 2.0 $mW/cm^2$<br>0.6 V<br>$[Dye]_0$ = 20 mg/l<br>5 h | 200 W high- pressure mercury lamp | 90.6 | (Zhao et al. 2009) |

| | | | | | | |
|---|---|---|---|---|---|---|
| multiwall carbon nano-tubes- $TiO_2$/Ti | electrophoretic depo-sition | Acid Red 33 (AR33) | 7.5 mA/cm$^2$<br>60 min<br>pH = 5.2 | UV light source (280–400 nm) | 98 | (Nabizadeh Chianeh and Basiri Parsa 2015) |
| Cu-$TiO_2$ | anodizing and elec-trodeposition | Methyl orange | 0.5 V<br>$[Dye]_0$ = 3.0 ppm<br>10 min | UV and Vis irradiation | 92.88 | (Nurdin et al. 2021) |

358

## 4. Photoelectro-Fenton and Solar Photoelectro-Fenton

Photoelectro-Fenton is a modernization of the EF process by irradiation with UV or sunlight, or photoexcitation with visible light of $Fe^{3+}$ complexes with carboxylic acids formed in the Fenton reaction (equation (9) for the regeneration of $Fe^{2+}$ with the formation of •OH (equations (11) and (12)), thus increasing the amount and regeneration of •OH, as well as the efficiency of the process (Vasudevan and Oturan 2014; Sirés et al. 2014b; Brillas and Martínez-Huitle 2015; Nidheesh et al. 2018; Brillas 2020). The photogenerated $Fe^{2+}$ ion can subsequently catalyzed the Fenton reaction with the formation of $Fe^{3+}$ and ring closure (equation (9)).

$$Fe^{2+} + H_2O_2 + H^+ \rightarrow Fe^{3+} + \bullet OH + H_2O \quad (9)$$

$$Fe^{3+} + H_2O \rightarrow Fe(OH)^{2+} + H^+ \quad (10)$$

$$Fe(OH)^{2+} + h\nu \rightarrow Fe^{2+} + \bullet OH \quad (11)$$

$$Fe(OOCR)^{2+} + h\nu \rightarrow Fe^{2+} + CO_2 + R\bullet \quad (12)$$

The high oxidation effect in the PEF is due to the action of hydroxyl radicals generated in situ under UV or solar irradiation in wastewater (Salazar et al. 2019a). This process is more effective for the complete mineralization of synthetic azo dyes and treatment of real wastewater (Wang et al. 2008; Almeida et al. 2012; Bedolla-Guzman et al. 2016).

The PEF has shown high efficiency to removal of azo dyes from wastewater. In the PEF and SPEF oxidation of azo dyes, hydrogen peroxide $H_2O_2$ is formed in dye solutions due to two-electron reduction of $O_2$ on cathode materials. The presence of small amounts of $Fe^{2+}$ leads to an increase the oxidation of azo dyes due to the formation of •OH and $Fe^{3+}$ in the bulk solution according to the Fenton reaction at the optimum pH ~ 3 (Sirés et al. 2014b). The use of sunlight in the PEF makes this technology inexpensive compared to the process using UV light. UV light contributes to the photoreduction of Fe $(OH)^{2+}$ according to reaction (11) with the regeneration of $Fe^{2+}$ and additional formation of • OH and the occurrence of the destruction reaction of Fe (III)-carboxylate intermediates (12), which are are resistant to various oxidative processes (Brillas 2020).

Various groups of researchers have investigated the effectiveness of both the PEF and the SPEF for the removal of azo dyes. The comparative study of the destruction of the azo dye active yellow 160 (RY160) due to anodic oxidation with the simultaneous generation of $H_2O_2$ (AO-$H_2O_2$), EF, PEF was carried out (Bedolla-Guzman et al. 2016). BDD as an anode and an air-diffusion cathode to produce $H_2O_2$ with the addition of 0.50 mmol/$dm^3$ $Fe^{2+}$ were used. The mineralization efficiency of the processes increases in the range AO-$H_2O_2$ < EF< FEF (Márquez et al. 2020). This trend is explained by the predominant formation of hydroxyl radicals on the anode surface as a result of water oxidation and in the volume as a result of the Fenton reaction (Medrano-Rodríguez et al. 2020). When using PEF, 94% mineralization of the azo dye active yellow 160

was achieved after 360 minutes at 100 mA/cm$^2$ at an initial concentration of 0.167 mmol/dm$^3$ (Bedolla-Guzman et al. 2016). The discoloration and mineralization of 290 mg/l azo dye Sunset Yellow FCF (SY) under analogous conditions was studied (Moreira et al. 2013). The same comparison of the efficiency of oxidation processes was carried out when removing acid blue 29 with a concentration of 118 mg/l with BDD, Pt and Ti/$RuO_2$ anodes, where the highest efficiency of azo dye oxidation due to the SPEF was also observed in comparison with electrochemical oxidation with simultaneous generation of $H_2O_2$ and EF process. After 15 min with the current dencity of 33.3 mA/cm$^2$, almost complete degradation of acid blue 29 was achieved, regardless of the anode used, and after 285 min, complete mineralization according to TOC was achieved (Fajardo et al. 2019). The combination of a gas-diffusion cathode and a DBA under sunlight irradiation leads to the same effect of removing azo dyes as when using UV light, which makes the use of the SPEF economically advantageous (Paz et al. 2020).

In some cases, SPEF can be supplemented by a process of continuous electrochemical generation of hypochlorous acid (HClO) and photoregeneration of Fe(II) with the formation of hydroxyl radicals. The presence of chloride ions in the electrolyte and the use of DSA anodes leads to the formation of HClO, which is involved in the oxidation of azo dyes (Murrieta et al. 2020). The use of anodes (DSA type) and an air-diffusion cathode connected to a solar photoreactor made it possible to completely mineralize the Acid Blue 29 dye using SPEF (Salazar et al. 2019b). Comparison of the efficiency of the SPEF process for processing solutions of acid red 1 in an electrolyte containing chlorides showed that in the PEF process a faster removal of color occurs compared to the process with the generation of HClO. The simultaneous implementation of both processes leads to a slightly faster discolouration than at the PEF (Titchou et al. 2022).

Congo red diazo dye under these conditions at 100 mA/cm$^2$ is completely mineralized at 240 minutes with a current efficiency of about 49% and 0.45 kWh/(g DOC) energy consumption (Solano et al. 2015). Azo dyes are removed mainly by the OH formed at the anode as a result of water oxidation and in the bulk solution as a result of the Fenton reaction between $Fe^{2+}$ and $H_2O_2$ generated at the cathode, as well as as a result of photolysis of $Fe(OH)^{2+}$ particles by light (Moreira et al. 2013). When $Fe^{2+}$ is added with the simultaneous generation of hydrogen peroxide at the cathode, the pH of the solution under optimal conditions should correspond to acidic values. This conclusion was made by the authors of works (Almeida et al. 2015; Elumalai et al. 2022), where the oxidation of active yellow 186 and orange G azo dyes was studied. The kinetics of the photo-electro-Fenton oxidation of azo dyes corresponds to the pseudo-first order (Brillas and Garcia-Segura 2016).

In the case of using iron electrodes for the oxidation of azo dyes, the generation of $Fe^{2+}$ and $H_2O_2$ occurs directly during the PEF (Moradi et al. 2015). In this case, a combination of electrocoagulation and PEF to remove azo dyes is the most appropriate option. Oxidation of Acid Blue 29 (AB 29) in an electrochemical filter press reactor equipped with a Ti|Ir-Sn-Sb oxide anode and stainless steel cathode plates achieved 62% discolouration and 84% COD removal (Márquez et al. 2022a). The combination of the electrocoagulation process makes it possible to treat highly concentrated azo dyes wastewater. The main part of the dye is removed due to the electrocoagulation process, and the dye remaining in the solution can be oxidized to $CO_2$ due to the PEF (Márquez et al. 2022b). The mineralization of the azo dyes Acid Violet 7 (AV7) and RB5 was studied using a photoelectro-Fenton process using a glassy carbon mesh electrode (cathode) and a steel mesh as anode (Salazar and Ureta-Zañartu 2012). Simultaneous generation of hydroxyl radicals on a $TiO_2$/Ti photocatalyst and in situ generation of Fenton's reagent on a stainless steel electrode significantly increases the efficiency of the removal of azo dyes, for example, orange G (Liu et al. 2019a). It should be noted that the hybrid process of electrocoagulation with PEF can be an alternative to conventional PEF in solutions containing a significant amount of chloride ions (Márquez et al. 2022b).

The mineralization of the azo dye Acid Red 14 was studied using the PEF in a single-chamber electrochemical reactor with a $RuO_2$/Ti anode and an activated carbon fiber cathode to generation of $H_2O_2$ electrochemically. Research results have shown that the EF process yields about 60–70% mineralization of AR14, while the PEF can mineralize AR14 more efficiently (removal of more than 94% TOC) even at low current densities after 6 hours of electrolysis (Wang et al. 2008). The combination of a photocatalytic process on $TiO_2$ nanoparticles with PEF during the oxidation of CI Basic Red 46 (BR46) and CI Acid Red 17 (AR17), as well as a mixture of azo dyes, leads to their complete mineralization according to TOC (Khataee et al. 2010a, 2012; Zarei et al. 2010). At the same time, the efficiency of mineralization decreases in the range PEF/$TiO_2$>PEF>EF>UV/$TiO_2$. The use of additional sonication makes it possible to further increase the rate of oxidation of azo dyes (Mahmoudi et al. 2022).

The presence of $Fe^{2+}$ ions is necessary for the oxidation of azo dyes in the PEF process. To avoid the use of iron salts as precursors for the homogeneous Fenton process, it is proposed to add iron compounds to the solution of azo dyes or to precipitate zero-valent iron on various substrate. The addition of heterogeneous catalysts containing iron compounds to the solution of azo dyes during the PEF leads to additional occurrence of heterogeneous Fenton-like processes (Isaev and Magomedova 2022). The results of studies to the removal of SY due to the SPEF showed that the discoloration of the solution is 98.7%, and the removal of TOC is 71% in 90 min of photoelectrolysis (Pinheiro et al. 2020). The mechanism of azo dye oxidation is shown on Fig. 3. The deposition

of zero-valent iron on various substrate with a large specific surface, which can be used as cathode materials, in particular, on activated carbon, promotes an additional occurrence of a heterogeneous photo-Fenton process during the oxidation of azo dyes (Ramírez et al. 2010; Bañuelos et al. 2015). Iron oxalates can also be used as catalysts for the decomposition of $H_2O_2$ during the oxidation of azo dyes in PEF (Khataee et al. 2010b). Comparison of the rate of oxidation of active red 195 showed that the removal of the color of the solution follows in descending order: PEF/oxalate > PEF > EF (Djafarzadeh et al. 2013).

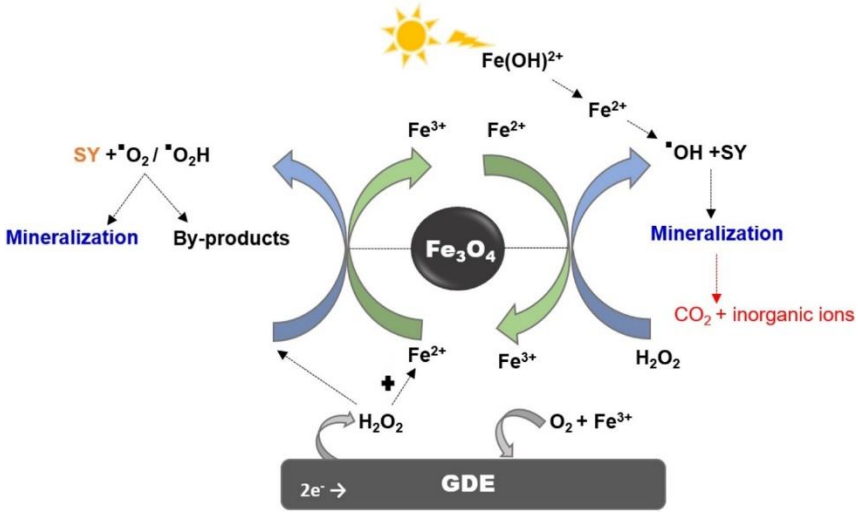


Fig. 3. The mechanism of oxidation of the SY dye due to the solar photoelectro-Fenton process in the presence of $Fe_3O_4$. Reprinted by permission from (Pinheiro et al. 2020). Copyright 2020, Elsevier.

The efficiency of oxidation of azo dyes by the PEF process is affected by such operating parameters as current density, solution pH, flow rate, initial $Fe^{2+}$ concentration, initial dye concentration, etc. (Zhang et al. 2011; Ruiz et al. 2011b; Khataee et al. 2013; Aveiro et al. 2018). The material of the anode and cathode also play an important role in the oxidation of azo dyes by the PEF process (Pereira et al. 2016; Wang et al. 2022). For example, Paz E.C. et al. (Paz et al. 2018) a new catalyst for the efficient generation of hydrogen peroxide using tungsten oxide as an additive was proposed, which was used in the oxidation of orange II and which showed high $H_2O_2$ current efficiency and low energy consumption. The rate of oxidation of azo dyes in PEF depends on the number of azo bonds in the molecule. Comparison of the oxidation rate of AO7 monoazo dye, acid

red 151 diazo, and dispersed blue 71 triazo dye using SPEF showed that the mineralization rate decreased in the following order AO7>DS71>KK151. For AO7, mineralization up to 97% was achieved, while short-line carboxylic acids remained in the final solution. For two other azo dyes, a mineralization of 90–92% was achieved, and their final solutions contained undetected products that were more stable than carboxylic acids (Garcia-Segura and Brillas 2016). Mahmoudi N. et al. (Mahmoudi et al. 2022) studied the discoloration of two widely used textile dyes, acid black 172 and dispersed black 56, of the combined sonophotoelectro-Fenton process. A dye oxidation efficiency of 95.5% and a COD removal efficiency of 91.6% for Disperse Black 56 were obtained under optimal conditions pH 3, current density 2 $mA/cm^2$, dye concentration 200 ppm, and a treatment time of 30 min, and in the case of acid black 172, the treatment time was 50 minutes to achieve the same performance.

Recently, researchers have great attention to the removal of food azo dyes. This is because some food azo dyes can reason hyperactivity and allergies in children. These food azo dyes include food additives E122 (Carmoisine, CI 14720), E124 (Ponceau 4R, CI 16255), and E129 (Allura Red AC, CI 16035) (Thiam et al. 2015a). The decomposition of a mixture of food azo dyes E122, E124 and E129 was studied by the PEP under UV light irradiation using BDD (or Pt) as an anode and an air diffusion cathode. In a sulfate medium, all azo dyes showed rapid discoloration, but almost complete mineralization was achieved faster in PEF with BDD. At the presence of chloride ions in solution, the formation of stable chlorine derivatives slowed down the oxidation process (Thiam et al. 2015a). Comparative oxidation of the food monoazo dye tartrazine due to various electrochemical processes was shown in (dos Santos et al. 2018). For a better understanding of the role of oxidizing agents, comparative tests of anodic oxidation and electrogenerated $H_2O_2$ (AO-$H_2O_2$), EF and PEF were carried out. Anodic oxidation with generation of $H_2O_2$ showed a small rate of oxidizing power. EF led to partial mineralization due to the formation of molecules resistant to the action of •OH. By-products were destroyed in the SPEF process, which led to complete mineralization of tartrazine (dos Santos et al. 2018).

Comparison of the oxidation process of another food coloring Allura Red AC in sulfate medium containing 0.50 mM $Fe^{2+}$ was studied using SPEF and EF. EF treatment resulted in rapid discoloration but poor mineralization as most of the products were slowly degraded by •OH formed from the Fenton reaction between $Fe^{2+}$ and $H_2O_2$ generated on the air diffusion cathode. During EF, TOC decreased by 39% after 180 min, after which the Allura Red AC oxidation process slowed down and reached only 46% mineralization after 360 min. Almost complete mineralization (96%) was achieved after 240 min of SPEF, which can be explained by the rapid photolysis of non-oxidizing intermediates (Thiam et al. 2015b). The comparison of the oxidation of azo dyes by various Photoelectro-Fenton process are presented in Table 2.

523 Table 2. Comparison of the oxidation of azo dyes by Photoelectro-Fenton process

| Photoanode | Type of process | Azo dye | Process parameters | Light source | Discoloration/TOC* | Ref |
|---|---|---|---|---|---|---|
| Ti\|Ir-Sn-Sb-oxides | electro- coagulation (EC) and active chlorine-based photoelectro-Fenton-like | Acid Blue 113 | u = 24.2 cm/s, i = 15 mA/cm$^2$ 0.4 mM $Fe^{2+}$ | UV-A lamp | 100 | (Márquez et al. 2022b) |
| | sono-photo-electro-Fenton | Acid Black 172 Disperse Blue 56 | $[Dye]_0$ = 125 mg/l, pH 5, i = 4 mA/cm$^2$ | UV lamp | 95.5–97.4% | (Mahmoudi et al. 2022) |
| BDD | photoelectro-Fenton | Acid Red 1 | $[Dye]_0$ = 300 mg/l 0.05M $Na_2SO_4$ pH 3.0 0.50mM $Fe^{2+}$ i=16.6-66.6 mA/cm$^2$ | UVA lamp | 95.2 | (Wang et al. 2022) |
| BDD | photoelectro-Fenton in chloride and sulfate media | direct red 23 | i=5 mA/cm$^2$, 6 h, 75% $Na_2SO_4$ + 25% NaCl | UV irradiation | 100* | (Titchou et al. 2022) |

| | | | | | | |
|---|---|---|---|---|---|---|
| Ti anode | photo electro-Fenton | Reactive Yellow 186 | $[Dye]_0$ = 0.05–0.25 g/l, pH 2–9, Fe dosage 0.01–0.03 g/l, $H_2O_2$ = 0.1–0.5 g/l i = 0.1–0.5 mA/cm2) | UVA radiation | 99<br>94.82* | (Elumalai et al. 2022) |
| BDD | UVA photoelectro-Fenton<br>solar photoelectro-Fenton | Erythrosine B | $[Dye]_0$ = 100 mg/l<br>i = 20 mA/cm$^2$;<br>$[Fe^{2+}]$ = 0.1 mM;<br>pH 3; 50 mM $Na_2SO_4$, 2 h | UVA lamp<br>Solar Light | 100* | (Clematis and Panizza 2021) |
| | Solar photoelectro-Fenton process using Fe3O4 nanoparticles as a catalyst | Sunset Yellow | 0.13 M NaCl<br>0.1 M $Na_2SO_4$<br>pH 3.0<br>90 min | Solar light | 98,7<br>71* | (Pinheiro et al. 2020) |
| Ti\|RuO2 | photoelectro-Fenton | Methyl Orange | $[TOC]_0$ = 30 mg/1<br>50 mM $Na_2SO_4$<br>0.50 mM $Fe^{2+}$<br>pH 3.0<br>i = 20 mA/cm$^2$ | UVA lamp | 100 at 30 min<br>94* at 240-300 min | (Márquez et al. 2020) |

| | | | | | | |
|---|---|---|---|---|---|---|
| BDD | simulated solar photoelectro-Fenton | Orange II | $[Dye]_0$ = 0.26 mM<br>0.1M $K_2SO_4$<br>pH 3.0<br>150 mA/$cm^2$ | Xe lamp | 93* | (Paz et al. 2020) |
| BDD | solar photoelectro-Fenton | Acid Blue 29 | $[Dye]_0$ = 118 mg/l<br>0.05 M $Na_2SO_4$<br>pH 3.0<br>0.5 mM $Fe^{2+}$<br>i = 33.3 mA/$cm^2$ | Sun light | 100 at 15 min<br>100* at 285 min | (Fajardo et al. 2019) |

524

## 5. Combined photoelectrochemical processes and reactors

Great interest in the photoelectrochemical oxidation of azo dyes, caused the appearance of various types of reactor designs for the process (Jaramillo-Gutiérrez et al. 2020) . Photoelectrocatalysis and related reactor designs have already been considered and discussed in some reviews (Meng et al. 2015; McMichael et al. 2021; Divyapriya et al. 2021). In recent years, great efforts have been made to bring the industrial application of photoelectrocatalysis out of its infancy and introduce this technology into production. In this regard, new types of reactors have been proposed based on new materials that are more efficient for oxidation of azo dyes and do not depend on their nomenclature. The main components of the installation for the photoelectrochemical oxidation of azo dyes are the reactor, where the photoelectrochemical reaction takes place, the light source and the power supply.

Reactors for photoelectrochemical removal of azo dyes can operate in batch, semi-batch and flow (continuous mode). Basically, all research and reactors that are used to remove azo dyes are currently at the level of laboratory developments. Fig. 4a shows a laboratory operating in a semi-batch mode and consisting of a polymethyl methacrylate tube with a bottom water inlet and a top outlet, a UV source surrounded by a titanium dioxide mesh (anode), and a steel mesh acting as a counter electrode (cathode) (Franz et al. 2015). A modular type reactor equipped with up to 9 separate photo-electrochemical cells is shown in Fig. 4b. In an individual cell, a TiO2 electrode deposited on a conductive glass substrate was used as a photoanode, and a stainless steel plate at a distance of 0.1 cm from the photoanode served as a cathode. The light source was either a UVA lamp placed behind the photoelectrode or sunlight using manual tilt and azimuth tracking (Shinde et al. 2009).

A new three-dimensional photoelectrocatalytic reactor (3D-PER) for the removal of dyes from wastewater, the scheme of which is shown in Fig. 4d, is proposed by Meng H.S. et al (Meng et al. 2021) . The outer structure is a cylindrical tank. A titanium plate (diameter 62 mm) fixed at the bottom of the reactor was used as an anode. An annular titanium grid located above the anode served as the cathode. A quartz U-shaped tube was placed in the middle of the reactor, inside which a high-pressure mercury lamp was fixed. Granular carbon was placed in one layer between the cylindrical container and the quartz U-shaped tube. Air was purged from the bottom of the reactor using an aeration pump. The bleaching efficiency of the dye solution was more than 95%; granular carbon showed stable characteristics when processed for 11 continuous cycles (Meng et al. 2021).

Blowing oxygen or air through the photoelectrochemical reactor leads to the reduction of oxygen to hydrogen peroxide, which increases the efficiency of removing azo dyes. Using this concept, an industrial prototype was developed with four identical reactors for the implementation of the PEF (Fig. 4c). $H_2O_2$ is formed electrochemically in the first stage by reduction of dissolved

oxygen. Then, in a second step, $H_2O_2$ is passed through an iron-catalyst column irradiated with UV light to stimulate the formation of hydroxyl radicals, which are added to an aqueous solution of Orange-II azo dye. The decolorization efficiency of Orange II solution ranged from 75% to 96% at pH 3-5 (Robles et al. 2017).

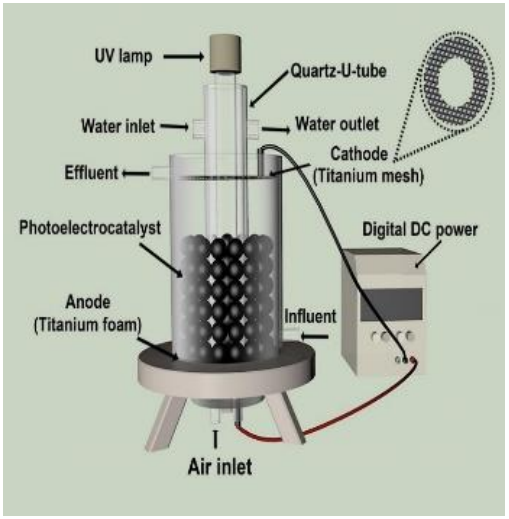


**a**

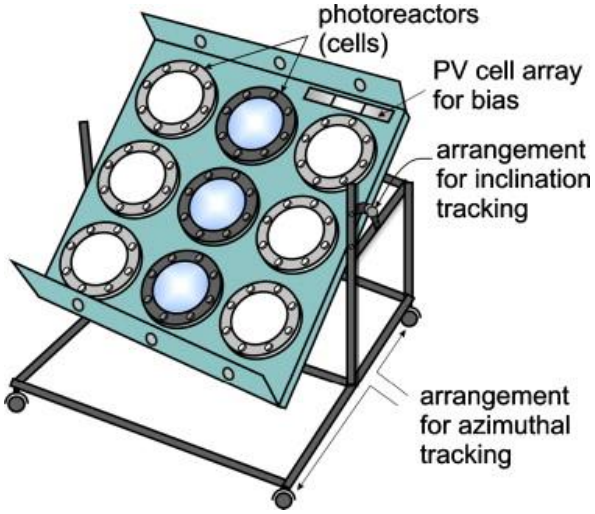


**b**

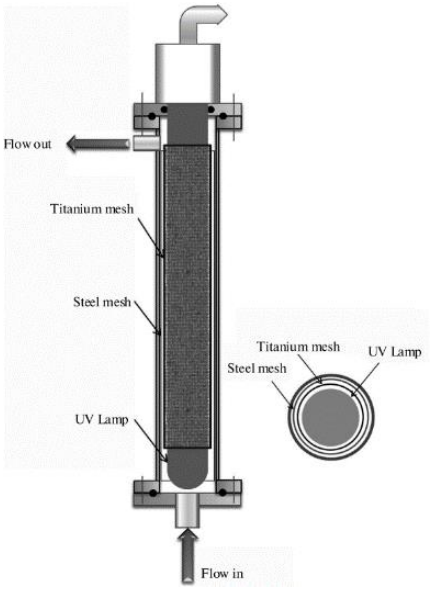


**c**

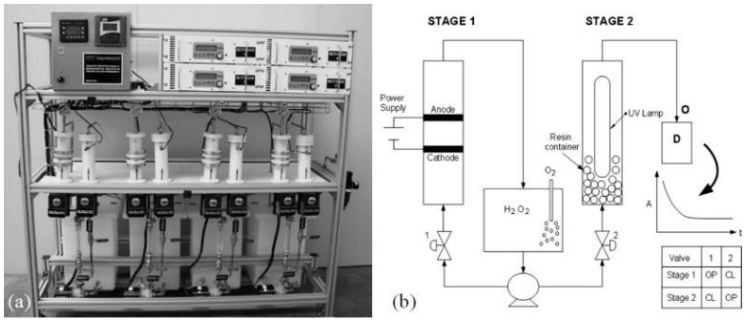


**d**

Fig. 4. a) – Photoelectrochemical semi-batch mode module for azo dye removal. Reprinted by permission from (Shinde et al. 2009). Copyright 2021, Elsevier; b) – modular type reactor equipped with up to 9 separate photo-electrochemical cells. Reprinted by permission from (Franz et al. 2015). Copyright 2009, Elsevier; c) – three-dimensional photoelectrocatalytic reactor Reprinted by permission from (Meng et al. 2021). Copyright 2015, Springer; d) – industrial prototype for producing an oxidant solution (a) and schematic description of the system, along with a two-stage process for producing an oxidant-rich aqueous solution (b). Reprinted by permission from (Robles et al. 2017). Copyright 2017, Elsevier.

The classic reactor for photoelectrochemical oxidation of azo dyes is a reservoir with two electrodes, a photoanode and a cathode, a radiation source and a power source, to support the required temperature, the reactor is in some cases equipped with a "jacket" around the reactor (Huda et al. 2019). A reactor with two electrodes is most often performed with undivided anode and cathode spaces. Photoanodes based on $TiO_2$ (Turolla et al. 2018; De Vidales et al. 2022; Chen et al. 2022a), BDD (Espinoza et al. 2016) are used as anodes, and carbon-based materials are used as cathodes. The main function of cathodes is the electrochemical reduction of oxygen to produce $H_2O_2$ (Chen et al. 2022a). In the case of the implementation of the PEF process, the cathode material plays a key role in the efficiency of the oxidation of azo dyes. As a cathode, materials with a large specific surface area, such as graphite felt and carbon cloth, are most often used (Thor et al. 2021). Semiconductors can also be used as cathodes. In this case, both electrode processes perform a useful function. A laboratory cell for photoelectrocatalysis using a $Cu_2O$ photocathode and a $WO_3/BiVO_4$ photoanode was developed for the simultaneous production of H2 and decomposition of organic dyes (Thongthep et al. 2021). The efficiency of azo dye oxidation can be increased by about 50% due to additional destruction at the cathode, as demonstrated in work (Xu et al. 2013).

In some cases, it is proposed to use a two-chamber electrolyzer. Lian Z. et al. (Lian et al. 2020) used a laboratory reactor made of quartz glass and divided into two chambers by a Nafion cation-exchange membrane to oxidize MO. Basically, two-chamber electrolyzers are used for laboratory studies in determining the magnitude of the applied voltage to the photoanode (Diao et al. 2013). Oxidation of active red 106 in a photoelectrocatalytic flow microreactor, where a tubular $TiO_2$ electrode was used as a partition separating the anode and cathode spaces and which simultaneously served as a photoanode, with a maximum degree of oxidation in the anode chamber of 80% of the initial dye concentration and 63 % dye in the cathode chamber was studied Suhadolnik L. et al (Suhadolnik et al. 2019).

An annular reactor with simultaneous air bubbling with a $TiO_2$ nanotube photoanode was studied Cardoso J.C. et al. (Cardoso et al. 2015) by the course of photoelectrochemical purification of real wastewater containing dyes. To implement the process of photoelectrochemical oxidation of azo dyes in a flow mode, a tubular design of the reactor is mainly used (Jaramillo-Gutiérrez et al. 2020). In the case of using solar energy to implement the photoelectrofenton process, the reactors for the oxidation of azo dyes are equipped with solar collectors (Garcia-Segura and Brillas 2014).

To achieve a more efficient removal of azo dyes, it was proposed to use combined photoelectrocatalysis with adsorption or filtration processes (Zhang et al. 2023). The combination of photoelectrocatalysis and membrane filtration is currently considered an attractive technology for

wastewater purification from organic compounds (Cheng and Han 2016). The creation of a reactor in which both filtration and photoelectrocatalysis can occur simultaneously is a rather difficult task due to the need to create a connection between the catalyst and a conductive substrate with effective filtering properties (Martins et al. 2020). In connection with this, research is being carried out on reactors with various membranes for the photoelectrochemical oxidation of dyes. As conducting porous membranes, it is proposed to use stainless steel membranes coated with $TiO_2$ and ZnO semiconductor oxides (Kumari et al. 2022, 2023). A sandwich membrane consisting of nylon fiber and stainless steel mesh with electro-deposited $WO_3$ showed high efficiency in photoelectrocatalytic wastewater treatment from active red dye 120. Complete removal of the dye was achieved after 150 min by passing an aqueous solution of active red for 120 s concentration of 10-5 mmol/l, pH = 4.0 and voltage of 1.0 V at a rate of 160 ml/min (Martins et al. 2020). The combination of microfiltration technology and photoelectrocatalysis with a conductive $TiO_2$/polyaniline (PANI)/polyvinylidene fluoride (PVDF) membrane, when irradiated with sunlight, significantly improves the decolorization efficiency of the azo dye (Sboui et al. 2022). The transfer of reagent molecules through membrane pores under pressure in the cross-flow filtration mode additionally facilitates the contact of the pollutant with catalytically active centers on and across membrane pores during photoelectrocatalysis (Chin et al. 2011).

Membrane fouling in the implementation of combined photoelectrochemical purification with simultaneous filtration is one of the main problems. To solve this problem, it is proposed to use a composite conductive membrane based on PVDF, carbon black, and $TiO_2$. The combined process of FEC with microfiltration in the flow mode includes a FEC reactor, an illumination unit with a Xe-lamp, and a constant voltage unit (1.0 V) (Sboui et al. 2023). Schematic diagram of filtration based on $TiO_2$/CB/PVDF membrane is shown in Fig. 5.

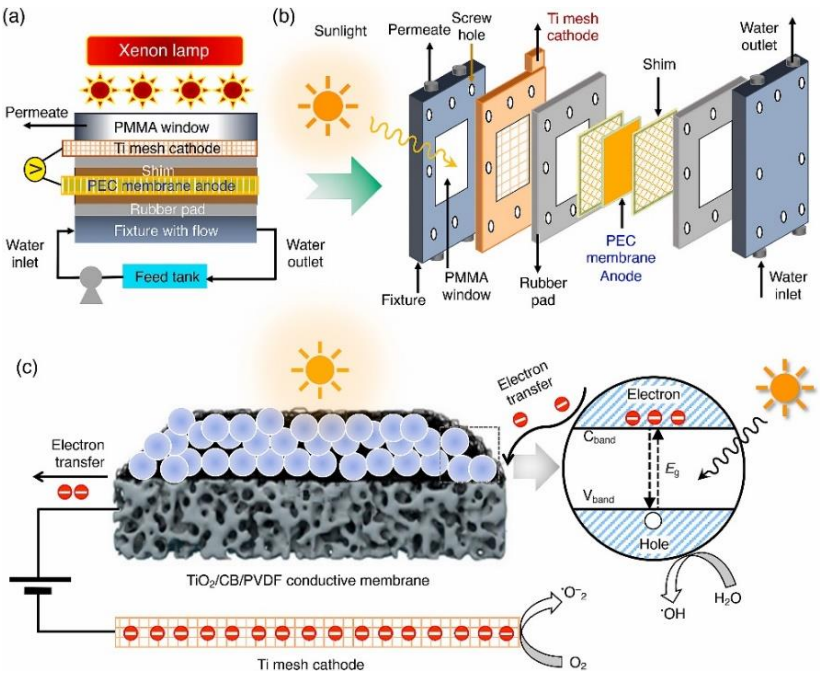


Fig. 5. Schematic diagrams of (a) the PEC membrane-based cross-flow filtration system; (b) the configuration of PEC membrane reactor with PEC membrane anode and Ti mesh cathode, and (c) PEC oxidization mechanism over $TiO_2$/CB/PVDF conductive membrane with electrochemical potential bias and $TiO_2$ charge transfer. Reprinted by permission from (Sboui et al. 2023). Copyright 2023, Elsevier.

The combination of photoelectrochemical oxidation of azo dyes with a fuel cell under UV or sunlight irradiation makes it possible to simultaneously purify wastewater and generate electricity (Antolini 2019). In this case, the energy generated in the fuel cell can be used to carry out photoelectrolysis. In this regard, the technology of microbial fuel cells (MFC) is proposed, which has the unique ability to convert organic substances in wastewater directly into electricity while treating wastewater (Janicek et al. 2015). In the MFC, electrons generated in the anode chamber by microorganisms due to separation from synthetic azo dyes as components of wastewater are transferred to the anode, and then, under the action of a difference in redox potentials, begin to move to the cathode, on which the reduction reactions proceed. Thus, electricity is produced along with the decomposition of pollutants. One of the ways to increase power generation in MFCs is the formation of a synergistic bioelectrophotocatalytic system. The recombination of photogenerated electron-hole pairs in such elements can be effectively reduced, resulting in more photogenerated electrons available for cathodic reduction reactions (Antolini 2019). However, a high cathode reduction reaction overvoltage is often the main limiting factor in MFC performance (Wei et al. 2011). A photoelectrocatalytic microbial fuel cell (photo-MFC) consisting of a p-type silicon

photocathode modified with Pd nanoparticles and a bioanode demonstrated the possibility of simultaneously generating electrical energy and decomposing the model azo dye MO. When illuminated with visible light, the photo-MFC showed an MO removal efficiency of 84.5% and a maximum output power density of 0.119. W/m2 for 36 h, which is twice as much as that of a conventional MFC with a carbon paper cathode (Han et al. 2017).

The cathodic destruction of RB5 with the simultaneous release of energy is effectively carried out in a two-chamber photo-MFC consisting of a bioanode and an AgBr/CuO hybrid photocathode both in bright light and in the dark. The characteristics of the composite are comparable with AgBr, CuO and pure graphite in terms of the specific MFC power, as well as its ability to decompose the ACh5 dye. The maximum efficiency of AF% destruction using an AgBr/CuO photocathode was 55.56% within 72 hours with a maximum power of 61.11 $mW/m^2$ (Ahmadpour et al. 2020). When using $TiO_2$ nanotubes as a photoanode in photo MFC, the reduction in COD was 56%, the degree of discoloration was 85% (Long et al. 2017). The use of an array of $TiO_2$ nanotubes also increases the generation of electric current from 3.64 ± 0.112 mA to 6.246 ± 0.135 mA (Long et al. 2019). When using MFC, the decomposition of azo dyes occurs mainly due to the reduction of dye molecules and oxidation by free radicals.

Another route of using combined methods of photoelectrochemical oxidation of azo dyes is their combination with the production of hydrogen at the cathode. Photoelectrochemical production of hydrogen and simultaneous destruction of organic compounds is a new route of research. On $Ti/TiO_2/WO_3$ under sunlight irradiation and optimal process conditions, it resulted in satisfactory hydrogen generation efficiency (46%) and dye removal (100% bleaching and 85% TOC reduction) (Guaraldo et al. 2016). The use of a heterostructure based on samarium vanadate ($SmVO_4$) and sulfur-doped carbon nitride (g-C3N4) as a photoanode showed a satisfactory efficiency of hydrogen generation with simultaneous photoelectrochemical oxidation of MO. The amount of hydrogen released during irradiation with sunlight was 22618 μmol/g-1 for 4 h. At the same time, the degree of discoloration for 80 min was 90% (Alkorbi et al. 2022).

To assess the profitability and overall performance of any treatment technology, an assessment of the energy consumption of the process is necessary. The research results showed that photolytic and photocatalytic processes require much more processing time and energy consumption (32 and 24 $kWh/m^3$, respectively) than the photoelectrocatalytic process (Ghasemian et al. 2017).

## 6. Azo dye oxidation products

Azo dyes are characterized by the presence of a functional azo group (-N=N-), with two or more symmetrical or asymmetric aromatic radicals (Bafana et al. 2011). The azo group can be

associated with benzene rings, naphthalene, aromatic heterocycles, or aliphatic groups, which impart color to the dye with different shades and intensities (Benkhaya et al. 2020). Currently, most dyes are not controlled for toxicity and are considered non-toxic. However, supposedly non-toxic azo dyes have functional groups that can impart mutagenic and carcinogenic properties when degraded (for example, compounds such as β-naphthylamine, aniline, triazine, p-phenylenediamine, β-amino-α-naphthol, which are known genotoxicants (Brüschweiler et al. 2014; Rawat et al. 2016)). It should also be noted that of the majority of azo dyes studied for toxicity, diazo, triazo, and polyazo dyes turned out to be more toxic (Golka et al. 2004). When assessing the toxicity of azo dyes, their possible destruction under the influence of various environmental factors is not taken into account, paying attention only to a laboratory study of toxicity. In addition, the microbiota of the animal's organism, including skin or intestinal microflora, can convert non-toxic azo dyes into carcinogenic metabolites (Feng et al. 2012). The formation of toxic decomposition products of azo dyes has been shown in many works (Brüschweiler et al. 2014). In particular, the authors (Golka et al. 2004) showed the formation of carcinogenic 3,3'-dimethoxybenzidine during the decomposition of the azo dye Direct blue 15 (Gottlieb et al. 2003). Analysis of the chemical structure of azo dyes showed that mutagenicity depends on the nature and position of halogen substituents both to aromatic rings and to the nitrogen atom of the amino group (Carneiro et al. 2010). When azo dyes, such as Disperse Blue 291, are oxidation using chlorine in solution, the formation of chlorinated products can occur, which are more toxic than the original dye. However, photoelectrochemical treatment reduces the mutagenicity of a solution containing CI Disperse Blue 291 (Carneiro et al. 2010). Based on this, one of the main tasks of the photoelectrochemical oxidation of azo dyes should be to reduce their toxicological properties.

Another problem of dye oxidation is to remove the color of solutions, which affects the biochemical processes in water bodies. In different works, high-performance liquid chromatography and mass spectrometry were mainly used to identify the products of oxidation of azo dyes (Huda et al. 2019), and for the characterization and genotoxicity, cytotoxicity, and mutagenicity of both initial solutions of azo dyes and solutions after photoelectrochemical treatment used the method of analysis of DNA comets, micronuclei and cytotoxicity in HepG2 cells, as well as analysis of mutagenicity using Salmonella (Ferraz et al. 2013).

At the photoelectrochemical oxidation of dyes, the destruction of the chromophore group occurs first, in the case of azo dyes, this is the -N=N- azo bond. Aromatic fragments of the azo dye molecule are formed as bond breaking products. For example, during the oxidation of RB5, fragments containing benzene rings and naphthalene structures are formed, and the solution becomes completely colorless, although the COD and TOC values are still at a high level (Liu et al. 2021). The initial nitrogen of the dye is mainly mineralized to the $NO_3^-$ ion and, to a lesser extent, to the

$NH_4^+$ ion, and the initial sulfur is converted to the $SO_4^{2-}$ ion (Solano et al. 2015; Garcia-Segura and Brillas 2016; Wang et al. 2022). Nitrogen contained in the azo dye molecule accumulates in the solution after photoelectrochemical treatment in the oxidation of acid blue 29 mainly in the form of $NO_3^-$, with an insignificant content of $NO_2^-$ and $NH_4^+$ (Fajardo et al. 2019).

The main products of the oxidation of azo dyes using different approaches are carboxylic acids, such as p-benzoquinone, maleic, fumaric, tartaric, tartaric, acetic, oxalic, oxamic, and formic acids (Almeida et al. 2012; Ghalebizade and Ayati 2016; Subba Rao et al. 2017). At the same time, carboxylic acids are also completely removed during longer processing. Oxalic acid, which accumulates in large amounts, is rapidly oxidized during photolysis of Fe(III)–oxalate complexes under UV or sunlight irradiation, while tartronic and oxamic acids are the most stable by-products due to the greater stability of their Fe(III)–oxalate complexes (Almeida et al. 2012). Chloride, sulfate, ammonium ions and, to a lesser extent, nitrate ions are the main mineral products of azo dye oxidation, which are released into solution from azo dye heteroatoms (Macedo et al. 2007; Brillas and Garcia-Segura 2016; Bedolla-Guzman et al. 2016).

The formation of carboxylic acids during the oxidation of acid blue 29 was studied by HPLC. Chromatograms showed well-defined peaks corresponding to acetic, formic, maleic and oxalic acids (Fajardo et al. 2019). Acetic and maleic acids are formed upon cleavage of the benzene rings of the diazo dye (do Vale-Júnior et al. 2018), and formic and oxalic acids upon the oxidation of longer carboxylic acids with subsequent mineralization to $CO_2$ and $H_2O$ (de Queiroz et al. 2017). The maximum accumulation of maleic and formic acids was observed after 120 min of treatment with a subsequent decrease in their content (Fajardo et al. 2019).

The main intermediates during Acid Red 88 and Direct Yellow 12 oxidation are various aromatic compounds and carboxylic acids (Table 3). The oxidation of the azo dye SY using PEF revealed 14 aromatic products and 34 hydroxylated derivatives, including compounds of benzoic, naphthalic, and phthalic acids. At the same time, carboxylic acids, such as tartronic, oxalic, formic, and oxamic, were also found (Moreira et al. 2013). For another dye, Congo red, the formation of 21 aromatic intermediates and 13 hydroxylated derivatives was identified, including compounds of diazo, monoazo, biphenyl, benzene, naphthalene, and phthalic acid (Solano et al. 2015). During PEF, the presence of iron ions leads to the formation of Fe(III)-carboxylate complexes, which are also subject to rapid destruction in the case of photostimulated processes (Ruiz et al. 2011a). After oxidation products of food azo dyes such as E122 (Carmoisine, CI 14720), E124 (Ponceau 4R, CI 16255) and E129 (Allura Red AC, CI 16035), 18 aromatic intermediates where identified by GC-MS and 6 short linear carboxylic acids using ion-exclusion HPLC (Thiam et al. 2015a).

760 Table 6. Intermediates of azo dye degradation products identified by various methods.

| Azo dye | Intermediates | Structure | Process parameters | Detection method | Ref |
|---|---|---|---|---|---|
| Acid Red 88 | 3-Sulfo-benzoic acid | 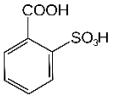 | Photoelectrocatalytic degradation under solar light irradiation, pH – 7, bias potential – 1.6 V, 5 mg/l NaCl | HPLC | (Olya et al. 2013) |
| | 4-Hydroxy-phthalic acid | 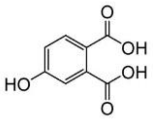 | | | |
| | Benzene |  | | | |
| | Naphthalene-1-sulfonic acid | 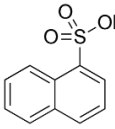 | | | |
| | Naphthalen-2-ol | 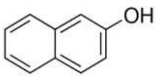 | | | |
| Direct Yellow 12 | 3-Ethoxy benzoic acid | 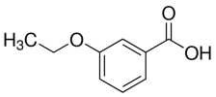 | Photoelectro-Fenton combined with photocatalytic process under UV-light irradiation, initial amount of Fe(III) 0.2 mM, initial dye concentration 50 mg/l, reaction time 70 min and applied current 400 mA | GC–MS | (Khataee and Zarei 2011) |
| | 4-Ethoxy phenol | 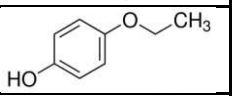 | | | |
| | Hydroquinone | 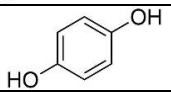 | | | |
| | 4-Ethoxy benzenamine | 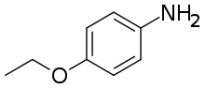 | | | |
| | Ethanedioic acid | 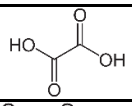 | | | |
| | Butendioic acid | 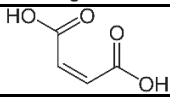 | | | |

761

762

763

764 ## 7. Conclusions

765 Azo dyes are one of the large classes of water-soluble dyes. Some food azo dyes have
766 shown toxicological and health effects in humans. Therefore, there is a need to develop methods
767 for their removal from aqueous solutions. The studies carried out over the past decades on the
768 photoelectrochemical oxidation of azo dyes have shown the potential applicability of this technol-
769 ogy for the treatment of wastewater containing azo dyes. Photoelectrochemical methods include
770 the advantages of both electrochemical and photocatalytic oxidation of azo dyes, showing a syn-

ergistic effect. The main advantage of photoelectrocatalysis compared to conventional photocatalysis is the suppression of the recombination of e-/h+ pairs due to the applied voltage, which leads to an increase in the concentration of charge carriers. Much attention of researchers is currently focused on the synthesis and use of corrosion-resistant semiconductors with a high efficiency of solar light conversion. In the case of photoelectrochemical oxidation of azo dyes, semiconductor materials are used in the form of electrodes, and in this case there is no need to clean the treated wastewater from particles, as in the case of a photocatalytic process. The use of sunlight makes the use of photoelectrochemical methods for the removal of azo dyes economically feasible. In this aspect, the preparation and study of new semiconductor catalysts that absorb daylight in the entire range of the sunlight spectrum is a direction for future research. The most promising for the removal of azo dyes are photo-electro-Fenton methods using solar light, which can be implemented at relatively low energy costs and a high rate of COD and TOC removal. In most cases, during the oxidation of azo dyes, carboxylic acids are formed as end products, followed by their mineralization to inorganic compounds. The combination of photoelectrochemical methods with other methods of azo dye removal, such as adsorption, membrane filtration, and fuel cells, is one of the promising areas of research in the field of azo dye removal. In general, most of the studies devoted to the photoelectrochemical removal of azo dyes from aqueous solutions are at the level of laboratory developments. The schemes of reactors given in the works refer to laboratory prototypes. At present, the question of the influence of the structure of azo dye molecules on the efficiency of their oxidation using photoelectrochemical methods (photoelectrocatalysis, photo-electro-Fenton, solar photo-electro-Fenton) remains unexplored. Photoelectrochemical oxidation of azo dyes leads only to discoloration of growth solutions with the formation of various aromatic structures. In this regard, there is a more detailed study of the decrease in the toxicological properties of azo dye solutions after photoelectrochemical treatment. Further research should be aimed at developing industrial technologies for treating real wastewater using photoelectrochemical oxidation using sunlight as an energy source.

**Funding**

There is no funding received for this research.

**Conflicts of interest/Competing interests**

The authors declare they have no financial interests.

**Ethics approval** (include appropriate approvals or waivers)

This study does not require ethics approval

**Availability of data and material** (data transparency)

Availability of data and material is not applicable to this article as no new data were created or analyzed in this study.

**Authors' contributions**

A. Isaev, N. Shabanov: Conceptualization, methodology, validation, formal analysis, writing original draft and review, visualization; M. Rabadanov: validation, writing—review and editing, supervision; Zhu Mingshan: conceptualization, methodology, validation, writing—review and editing, supervision.

## References

Ahmadpour T, Aber S, Hosseini MG (2020) Improved dye degradation and simultaneous electricity generation in a photoelectrocatalytic microbial fuel cell equipped with AgBr/CuO hybrid photocathode. J Power Sources 474:228589. https://doi.org/10.1016/J.JPOWSOUR.2020.228589

Ahmed EA, Abdessalam T, Aziz B, et al (2020) Photo-electrochemical degradation of wastewaters containing organics catalysed by phosphate-based materials: a review. Rev Environ Sci Bio/Technology 2020 194 19:843–872. https://doi.org/10.1007/S11157-020-09547-9

Ali T, Hunge YM, Venkatraman A (2018) UV assisted photoelectrocatalytic degradation of reactive red 152 dye using spray deposited $TiO_2$ thin films. J Mater Sci Mater Electron 29:1209–1215. https://doi.org/10.1007/S10854-017-8023-Y/FIGURES/7

Alimirzaeva ZM, Isaev AB, Shabanov NS, et al (2019) Photoelectrocatalytic activity $PbO_2$ loaded highly oriented $TiO_2$ nanotubes arrays. Mater Today Proc 36:325–327. https://doi.org/10.1016/j.matpr.2020.04.111

Alkorbi AS, Kumar KY, Prashanth MK, et al (2022) Samarium vanadate affixed sulfur self doped g-C3N4 heterojunction; photocatalytic, photoelectrocatalytic hydrogen evolution and dye degradation. Int J Hydrogen Energy 47:12988–13003. https://doi.org/10.1016/J.IJHYDENE.2022.02.071

Almeida LC, Garcia-Segura S, Arias C, et al (2012) Electrochemical mineralization of the azo dye Acid Red 29 (Chromotrope 2R) by photoelectro-Fenton process. Chemosphere 89:751–758. https://doi.org/10.1016/J.CHEMOSPHERE.2012.07.007

Almeida LC, Silva BF, Zanoni MVB (2015) Photoelectrocatalytic/photoelectro-Fenton coupling system using a nanostructured photoanode for the oxidation of a textile dye: Kinetics study and oxidation pathway. Chemosphere 136:63–71. https://doi.org/10.1016/J.CHEMOSPHERE.2015.04.042

Antolini E (2019) Photoelectrocatalytic fuel cells and photoelectrode microbial fuel cells for wastewater treatment and power generation. J Environ Chem Eng 7:103241. https://doi.org/10.1016/J.JECE.2019.103241

Aveiro LR, Da Silva AGM, Candido EG, et al (2018) Application and stability of cathodes with manganese dioxide nanoflowers supported on Vulcan by Fenton systems for the degradation of RB5 azo dye. Chemosphere 208:131–138. https://doi.org/10.1016/J.CHEMOSPHERE.2018.05.107

Ayoubi-Feiz B, Aber S, Khataee A, Alipour E (2014) Preparation and application of α-$Fe_2O_3$/$TiO_2$/activated charcoal plate nanocomposite as an electrode for electrosorption-

assisted visible light photoelectrocatalytic process. J Mol Catal A Chem 395:440–448. https://doi.org/10.1016/J.MOLCATA.2014.09.006

Azis T, Nurdin M, Riadi LS, et al (2021) Photoelectrocatalytic performance of ilmenite(FeTiO3) doped $TiO_2$/Ti electrode for reactive green 19 degradation in the UV-visible region. J Phys Conf Ser 1899:012041. https://doi.org/10.1088/1742-6596/1899/1/012041

Bafana A, Devi SS, Chakrabarti T (2011) Azo dyes: Past, present and the future. Environ Rev 19:350–370. https://doi.org/10.1139/a11-018

Bañuelos JA, García-Rodríguez O, Rodríguez-Valadez FJ, Godínez LA (2015) Electrochemically Prepared Iron-Modified Activated Carbon Electrodes for Their Application in Electro-Fenton and Photoelectro-Fenton Processes. J Electrochem Soc 162:E154–E159. https://doi.org/10.1149/2.0581509JES/XML

Bedolla-Guzman A, Sirés I, Thiam A, et al (2016) Application of anodic oxidation, electro-Fenton and UVA photoelectro-Fenton to decolorize and mineralize acidic solutions of Reactive Yellow 160 azo dye. Electrochim Acta 206:307–316. https://doi.org/10.1016/J.ELECTACTA.2016.04.166

Benkhaya S, M'rabet S, El Harfi A (2020) Classifications, properties, recent synthesis and applications of azo dyes. Heliyon 6:. https://doi.org/10.1016/j.heliyon.2020.e03271

Bessegato GG, De Almeida LC, Ferreira SLC, Zanoni MVB (2019) Experimental design as a tool for parameter optimization of photoelectrocatalytic degradation of a textile dye. J Environ Chem Eng 7:103264. https://doi.org/10.1016/J.JECE.2019.103264

Bessegato GG, Guaraldo TT, de Brito JF, et al (2015) Achievements and Trends in Photoelectrocatalysis: from Environmental to Energy Applications. Electrocatal 6:415–441. https://doi.org/10.1007/S12678-015-0259-9

Bilińska L, Gmurek M (2021) Novel trends in AOPs for textile wastewater treatment. Enhanced dye by-products removal by catalytic and synergistic actions. Water Resour Ind 26:100160. https://doi.org/10.1016/J.WRI.2021.100160

Brillas E (2020) A review on the photoelectro-Fenton process as efficient electrochemical advanced oxidation for wastewater remediation. Treatment with UV light, sunlight, and coupling with conventional and other photo-assisted advanced technologies. Chemosphere 250:126198. https://doi.org/10.1016/j.chemosphere.2020.126198

Brillas E, Garcia-Segura S (2016) Solar Photoelectro-Fenton Degradation of Acid Orange 7 Azo Dye in a Solar Flow Plant: Optimization by Response Surface Methodology. Water Conserv Sci Eng 2016 11 1:83–94. https://doi.org/10.1007/S41101-016-0005-Z

Brillas E, Martínez-Huitle CA (2015) Decontamination of wastewaters containing synthetic organic dyes by electrochemical methods. An updated review. Appl Catal B Environ 166–

167:603–643. https://doi.org/10.1016/J.APCATB.2014.11.016

Brüschweiler BJ, Küng S, Bürgi D, et al (2014) Identification of non-regulated aromatic amines of toxicological concern which can be cleaved from azo dyes used in clothing textiles. Regul Toxicol Pharmacol 69:263–272. https://doi.org/10.1016/j.yrtph.2014.04.011

Cao D, Wang Y, Zhao X (2017) Combination of photocatalytic and electrochemical degradation of organic pollutants from water. Curr Opin Green Sustain Chem 6:78–84. https://doi.org/10.1016/J.COGSC.2017.05.007

Cardoso JC, Lucchiari N, Zanoni MVB (2015) Bubble annular photoeletrocatalytic reactor with $TiO_2$ nanotubes arrays applied in the textile wastewater. J Environ Chem Eng 3:1177–1184. https://doi.org/10.1016/J.JECE.2015.04.010

Carneiro PA, Oliveira DP, Umbuzeiro GA, Zanoni MVB (2010) Mutagenic activity removal of selected disperse dye by photoeletrocatalytic treatment. J Appl Electrochem 40:485–492. https://doi.org/10.1007/S10800-009-0018-9/FIGURES/6

Castillo-Cabrera GX, Espinoza-Montero PJ, Alulema-Pullupaxi P, et al (2022) Bismuth Oxyhalide-Based Materials (BiOX: X = Cl, Br, I) and Their Application in Photoelectrocatalytic Degradation of Organic Pollutants in Water: A Review. Front Chem 10:. https://doi.org/10.3389/FCHEM.2022.900622

Cervantes TNM, Zaia DAM, Moore GJ, de Santana H (2013) Photoelectrocatalysis Study of the Decolorization of Synthetic Azo Dye Mixtures on Ti/$TiO_2$. Electrocatalysis 4:85–91. https://doi.org/10.1007/S12678-012-0123-0/TABLES/7

Chen T, Jin GP, Xu Z, et al (2022a) Improving generation of $H_2O_2$ and ·OH at bismuth hexacyanoferrate/graphene/carbon fibers-based gas diffusion electrode for degradation of dye wastewaters in photo-electro-Fenton process. Int J Environ Sci Technol 19:7941–7950. https://doi.org/10.1007/S13762-021-03533-6

Chen W, Liu S, Fu Y, et al (2022b) Recent advances in photoelectrocatalysis for environmental applications: Sensing, pollutants removal and microbial inactivation. Coord Chem Rev 454:214341. https://doi.org/10.1016/J.CCR.2021.214341

Cheng ZL, Han S (2016) Preparation of a novel composite electrode based on N-doped TiO2-coated NaY zeolite membrane and its photoelectrocatalytic performance. Chinese Chem Lett 27:467–470. https://doi.org/10.1016/J.CCLET.2015.12.010

Chin S, Park E, Kim M, et al (2011) Synthesis and photocatalytic activity of TiO2 nanoparticles prepared by chemical vapor condensation method with different precursor concentration and residence time. J Colloid Interface Sci 362:470–476. https://doi.org/10.1016/J.JCIS.2011.06.034

Clematis D, Panizza M (2021) Electro-Fenton, solar photoelectro-Fenton and UVA photoelectro-

Fenton: Degradation of Erythrosine B dye solution. Chemosphere 270:129480. https://doi.org/10.1016/J.CHEMOSPHERE.2020.129480

Cong Y, Li Z, Zhang Y, et al (2012) Fabrication of $Fe_2O_3/TiO_2$ Nanotube Electrode and Its Photoelectrocatalytic Performance in Dye Wastewater Degradation. Chinese J Catal 33:1402. https://doi.org/10.3724/SP.J.1088.2012.20429

Daghrir R, Drogui P, Robert D (2012) Photoelectrocatalytic technologies for environmental applications. J Photochem Photobiol A Chem 238:41–52. https://doi.org/10.1016/j.jphotochem.2012.04.009

de Queiroz JLA, da Silva ARL, de Moura DC, et al (2017) Electrochemical study of carboxylic acids with Nb-supported boron doped diamond anode. Part 1: Potentiodynamic measurements and bulk oxidations. J Electroanal Chem 794:204–211. https://doi.org/10.1016/J.JELECHEM.2017.04.006

De Vidales MJM, Palomo De La Fuente E, Atanes-Sánchez E, Fernández-Martínez F (2022) New compact multi option photo reactor for the removal of contaminants of emerging concern from wastewater. J Environ Chem Eng 10:107700. https://doi.org/10.1016/J.JECE.2022.107700

Deng X, Zhang H, Guo R, et al (2018) Effect of fabricating parameters on photoelectrocatalytic performance of $CeO_2/TiO_2$ nanotube arrays photoelectrode. Sep Purif Technol 193:264–273. https://doi.org/10.1016/J.SEPPUR.2017.10.066

Diao Z, Li M, Zeng F, et al (2013) Degradation pathway of malachite green in a novel dual-tank photoelectrochemical catalytic reactor. J Hazard Mater 260:585–592. https://doi.org/10.1016/J.JHAZMAT.2013.05.037

Divyapriya G, Singh S, Martínez-Huitle CA, et al (2021) Treatment of real wastewater by photoelectrochemical methods: An overview. Chemosphere 276:130188. https://doi.org/10.1016/J.CHEMOSPHERE.2021.130188

Djafarzadeh N, Zarei M, Behjati B, Khataee AR (2013) Optimization of the oxalate catalyzed photoelectro-Fenton process under visible light for removal of Reactive Red 195 using a carbon paper cathode. Res Chem Intermed 39:3355–3369. https://doi.org/10.1007/S11164-012-0848-7/TABLES/6

do Vale-Júnior E, da Silva DR, Fajardo AS, Martínez-Huitle CA (2018) Treatment of an azo dye effluent by peroxi-coagulation and its comparison to traditional electrochemical advanced processes. Chemosphere 204:548–555. https://doi.org/10.1016/J.CHEMOSPHERE.2018.04.007

dos Santos AJ, Sirés I, Martínez-Huitle CA, Brillas E (2018) Total mineralization of mixtures of Tartrazine, Ponceau SS and Direct Blue 71 azo dyes by solar photoelectro-Fenton in pre-

957 pilot plant. Chemosphere 210:1137–1144.
958 https://doi.org/10.1016/J.CHEMOSPHERE.2018.07.116
959 Elumalai G, Sowmya B, Rajan RK, Shanmugam V (2022) Experimental study of photo electro-
960 Fenton method for the removal of Reactive Yellow 186: Influence of operational
961 parameters. Environ Prog Sustain Energy e14061. https://doi.org/10.1002/EP.14061
962 Espinoza C, Romero J, Villegas L, et al (2016) Mineralization of the textile dye acid yellow 42
963 by solar photoelectro-Fenton in a lab-pilot plant. J Hazard Mater 319:24–33.
964 https://doi.org/10.1016/J.JHAZMAT.2016.03.003
965 Fajardo AS, dos Santos AJ, de Araújo Costa ECT, et al (2019) Effect of anodic materials on
966 solar photoelectro-Fenton process using a diazo dye as a model contaminant. Chemosphere
967 225:880–889. https://doi.org/10.1016/J.CHEMOSPHERE.2019.03.071
968 Fei W, Li H, Li N, et al (2020) Facile fabrication of ZnO/$MoS_2$ p-n junctions on Ni foam for
969 efficient degradation of organic pollutants through photoelectrocatalytic process. Sol
970 Energy 199:164–172. https://doi.org/10.1016/J.SOLENER.2020.02.037
971 Feng J, Cerniglia CE, Chen H (2012) Toxicological significance of azo dye metabolism by
972 human intestinal microbiota. Front Biosci (Elite Ed) 4:568. https://doi.org/10.2741/e400
973 Feng Z, Tian Q, Yang Q, et al (2021) Selectively photoelectrocatalytic reduction of oxygen to
974 hydroxyl radical and singlet oxygen: Mechanism and validation in coal wastewater. Appl
975 Catal B Environ 286:119908. https://doi.org/10.1016/J.APCATB.2021.119908
976 Ferraz ERA, Oliveira GAR, Grando MD, et al (2013) Photoelectrocatalysis based on Ti/$TiO_2$
977 nanotubes removes toxic properties of the azo dyes Disperse Red 1, Disperse Red 13 and
978 Disperse Orange 1 from aqueous chloride samples. J Environ Manage 124:108–114.
979 https://doi.org/10.1016/J.JENVMAN.2013.03.033
980 Florêncio J, Pacheco MJ, Lopes A, Ciríaco L (2013) Application of Ti/Pt/β-$PbO_2$ Anodes in the
981 Degradation of DR80 Azo Dye. Port Electrochim Acta 31:257–264.
982 https://doi.org/10.4152/pea.201305257
983 Fraga LE, Franco JH, Orlandi MO, Zanoni MVB (2013) Photoelectrocatalytic oxidation of hair
984 dye basic red 51 at W/$WO_3$/$TiO_2$ bicomposite photoanode activated by ultraviolet and
985 visible radiation. J Environ Chem Eng 1:194–199.
986 https://doi.org/10.1016/J.JECE.2013.04.018
987 Franz S, Perego D, Marchese O, Bestetti M (2015) Photoelectrochemical advanced oxidation
988 processes on nanostructured $TiO_2$ catalysts: Decolorization of a textile azo-dye. J Water
989 Chem Technol 37:108–115. https://doi.org/10.3103/S1063455X15030029
990 Fujishima A, Honda K (1972) Electrochemical Photolysis of Water at a Semiconductor
991 Electrode. Nat 1972 2385358 238:37–38. https://doi.org/10.1038/238037a0

992 Ganiyu SO, Martínez-Huitle CA, Oturan MA (2021) Electrochemical advanced oxidation
993 processes for wastewater treatment: Advances in formation and detection of reactive species
994 and mechanisms. Curr Opin Electrochem 27:100678.
995 https://doi.org/10.1016/J.COELEC.2020.100678
996 Ganiyu SO, Zhou M, Martínez-Huitle CA (2018) Heterogeneous electro-Fenton and
997 photoelectro-Fenton processes: A critical review of fundamental principles and application
998 for water/wastewater treatment. Appl Catal B Environ 235:103–129.
999 https://doi.org/10.1016/J.APCATB.2018.04.044
1000 García-Espinoza JD, Robles I, Durán-Moreno A, Godínez LA (2021) Photo-assisted
1001 electrochemical advanced oxidation processes for the disinfection of aqueous solutions: A
1002 review. Chemosphere 274:129957.
1003 https://doi.org/10.1016/J.CHEMOSPHERE.2021.129957
1004 Garcia-Segura S, Brillas E (2017) Applied photoelectrocatalysis on the degradation of organic
1005 pollutants in wastewaters. J Photochem Photobiol C Photochem Rev 31:1–35.
1006 https://doi.org/10.1016/J.JPHOTOCHEMREV.2017.01.005
1007 Garcia-Segura S, Brillas E (2016) Combustion of textile monoazo, diazo and triazo dyes by solar
1008 photoelectro-Fenton: Decolorization, kinetics and degradation routes. Appl Catal B Environ
1009 181:681–691. https://doi.org/10.1016/J.APCATB.2015.08.042
1010 Garcia-Segura S, Brillas E (2014) Advances in solar photoelectro-Fenton: Decolorization and
1011 mineralization of the Direct Yellow 4 diazo dye using an autonomous solar pre-pilot plant.
1012 Electrochim Acta 140:384–395. https://doi.org/10.1016/J.ELECTACTA.2014.04.009
1013 Ge MZ, Cao CY, Huang JY, et al (2016) Synthesis, modification, and
1014 photo/photoelectrocatalytic degradation applications of $TiO_2$ nanotube arrays: A review.
1015 Nanotechnol Rev 5:75–112. https://doi.org/10.1515/NTREV-2015-
1016 0049/ASSET/GRAPHIC/J_NTREV-2015-0049_CV_009.JPG
1017 Ghalebizade M, Ayati B (2016) Solar photoelectrocatalytic degradation of Acid Orange 7 with
1018 ZnO/$TiO_2$ nanocomposite coated on stainless steel electrode. Process Saf Environ Prot
1019 103:192–202. https://doi.org/10.1016/J.PSEP.2016.07.009
1020 Ghasemian S, Nasuhoglu D, Omanovic S, Yargeau V (2017) Photoelectrocatalytic degradation
1021 of pharmaceutical carbamazepine using Sb-doped Sn80%-W20%-oxide electrodes. Sep
1022 Purif Technol 188:52–59. https://doi.org/10.1016/J.SEPPUR.2017.07.007
1023 Golka K, Kopps S, Myslak ZW (2004) Carcinogenicity of azo colorants: influence of solubility
1024 and bioavailability. Toxicol Lett 151:203–210.
1025 https://doi.org/10.1016/J.TOXLET.2003.11.016
1026 Gottlieb A, Shaw C, Smith A, et al (2003) The toxicity of textile reactive azo dyes after

hydrolysis and decolourisation. J Biotechnol 101:49–56. https://doi.org/10.1016/S0168-1656(02)00302-4

Guaraldo TT, Gonçales VR, Silva BF, et al (2016) Hydrogen production and simultaneous photoelectrocatalytic pollutant oxidation using a $TiO_2/WO_3$ nanostructured photoanode under visible light irradiation. J Electroanal Chem 765:188–196. https://doi.org/10.1016/J.JELECHEM.2015.07.034

Han HX, Shi C, Yuan L, Sheng GP (2017) Enhancement of methyl orange degradation and power generation in a photoelectrocatalytic microbial fuel cell. Appl Energy 204:382–389. https://doi.org/10.1016/J.APENERGY.2017.07.032

He Y, Lin H, Guo Z, et al (2019) Recent developments and advances in boron-doped diamond electrodes for electrochemical oxidation of organic pollutants. Sep Purif Technol 212:802–821. https://doi.org/10.1016/J.SEPPUR.2018.11.056

Hepel M, Hazelton S (2005) Photoelectrocatalytic degradation of diazo dyes on nanostructured $WO_3$ electrodes. Electrochim Acta 50:5278–5291. https://doi.org/10.1016/J.ELECTACTA.2005.03.067

Huda A, Suman PH, Torquato LDM, et al (2019) Visible light-driven photoelectrocatalytic degradation of acid yellow 17 using Sn3O4 flower-like thin films supported on Ti substrate ($Sn_3O_4/TiO_2/Ti$). J Photochem Photobiol A Chem 376:196–205. https://doi.org/10.1016/J.JPHOTOCHEM.2019.01.039

Hunge YM, Yadav AA, Mahadik MA, et al (2018) Degradation of organic dyes using spray deposited nanocrystalline stratified $WO_3/TiO_2$ photoelectrodes under sunlight illumination. Opt Mater (Amst) 76:260–270. https://doi.org/10.1016/J.OPTMAT.2017.12.044

Isaev AB, Aliev ZM, Adamadzieva NA (2012) Photoelectrochemical oxidation of C.i. direct black 22 azo dye under elevated oxygen pressure. Russ J Appl Chem 85:765–769. https://doi.org/10.1134/S107042721205014X

Isaev AB, Magomedova AG (2022) Advanced Oxidation Processes Based Emerging Technologies for Dye Wastewater Treatment. Moscow Univ Chem Bull 77:181–196. https://doi.org/10.3103/S0027131422040046

Isaev AB, Shabanov NS, Orudzhev FF (2018) Influence of oxygen pressure to photoelectrochemical oxidation C.I. direct black 22 on $TiO_2$ nanotube array photoanode. Int J Environ Sci Technol 15:1609–1618. https://doi.org/10.1007/S13762-017-1523-8

Isaev AB, Shabanov NS, Sobola D, et al. (2022) ZnO/Chalcogenides Semiconductor Heterostructures for Photoelectrochemical Water Splitting. In Kaviyarasu K et al. (ed) Nanomaterials for Energy Conversion, Biomedical and Environmental Applications, Springer Nature, Singapore, pp. 3–35. https://doi.org/10.1007/978-981-19-2639-6_1

1062 Isaev AB, Tajibova NA, et al. (2013) Photoelectrocatalytic and photocatalytic oxidation of
1063 azodye at high oxygen pressure. J. Sib. Fed. Univ. Chem. 6:114–121
1064 Janicek A, Fan Y, Liu H (2015) Performance and stability of different cathode base materials for
1065 use in microbial fuel cells. J Power Sources 280:159–165.
1066 https://doi.org/10.1016/J.JPOWSOUR.2015.01.098
1067 Jaramillo-Gutiérrez MI, Carreño-Lizcano MI, Ruiz–Lizarazo JO, et al (2020) Design,
1068 mathematical modelling, and numerical simulation of a novel tubular photoelectrochemical
1069 reactor and experimental validation by residence time distribution and mass transfer
1070 coefficients. Chem Eng J 386:. https://doi.org/10.1016/J.CEJ.2019.123895
1071 Jiang D, Zhou T, Sun Q, et al (2011) Enhanced Visible-Light-Induced Photoelectrocatalytic
1072 Degradation of Methyl Orange by CdS Sensitized $TiO_2$ Nanotube Arrays Electrode.
1073 Chinese J Chem 29:2505–2510. https://doi.org/10.1002/CJOC.201180422
1074 Karanasios N, Georgieva J, Valova E, et al (2015) Photoelectrocatalytic Oxidation of Organics
1075 Under Visible Light Illumination: A Short Review. Curr Organic Chem 6:512-520
1076 https://doi.org/10.2174/1385272819666150115000247
1077 Karim A V., Nidheesh PV, Oturan MA (2021) Boron-doped diamond electrodes for the
1078 mineralization of organic pollutants in the real wastewater. Curr Opin Electrochem
1079 30:100855. https://doi.org/10.1016/J.COELEC.2021.100855
1080 Khataee AR, Safarpour M, Naseri A, Zarei M (2012) Photoelectro-Fenton/nanophotocatalysis
1081 decolorization of three textile dyes mixture: Response surface modeling and multivariate
1082 calibration procedure for simultaneous determination. J Electroanal Chem 672:53–62.
1083 https://doi.org/10.1016/J.JELECHEM.2012.03.010
1084 Khataee AR, Vahid B, Behjati B, Safarpour M (2013) Treatment of a dye solution using
1085 photoelectro-fenton process on the cathode containing carbon nanotubes under recirculation
1086 mode: Investigation of operational parameters and artificial neural network modeling.
1087 Environ Prog Sustain Energy 32:557–563. https://doi.org/10.1002/EP.11657
1088 Khataee AR, Zarei M (2011) Photoelectrocatalytic decolorization of diazo dye by zinc oxide
1089 nanophotocatalyst and carbon nanotube based cathode: Determination of the degradation
1090 products. Desalination 278:117–125. https://doi.org/10.1016/J.DESAL.2011.05.004
1091 Khataee AR, Zarei M, Asl SK (2010a) Photocatalytic treatment of a dye solution using
1092 immobilized TiO2 nanoparticles combined with photoelectro-Fenton process: Optimization
1093 of operational parameters. J Electroanal Chem 648:143–150.
1094 https://doi.org/10.1016/J.JELECHEM.2010.07.017
1095 Khataee AR, Zarei M, Moradkhannejhad L (2010b) Application of response surface
1096 methodology for optimization of azo dye removal by oxalate catalyzed photoelectro-Fenton

process using carbon nanotube-PTFE cathode. Desalination 258:112–119. https://doi.org/10.1016/J.DESAL.2010.03.028

Kumari P, Bahadur N, Conlan XA, et al (2022) Atomically-thin Schottky-like photo-electrocatalytic cross-flow membrane reactors for ultrafast remediation of persistent organic pollutants. Water Res 218:118519. https://doi.org/10.1016/J.WATRES.2022.118519

Kumari P, Bahadur N, Conlan XA, et al (2023) Stimuli-responsive heterojunctions based photo-electrocatalytic membrane reactors for reactive filtration of persistent organic pollutants. Chem Eng J 452:139374. https://doi.org/10.1016/J.CEJ.2022.139374

Kusmierek E (2020) Semiconductor Electrode Materials Applied in Photoelectrocatalytic Wastewater Treatment—an Overview. Catalysts 10:469. https://doi.org/10.3390/catal10040439

Kusmierek E, Chrzescijanska E (2015) Application of TiO2–RuO2/Ti electrodes modified with $WO_3$ in electro- and photoelectrochemical oxidation of Acid Orange 7 dye. J Photochem Photobiol A Chem 302:59–68. https://doi.org/10.1016/J.JPHOTOCHEM.2015.01.009

Laghrib F, Bakasse M, Lahrich S, El Mhammedi MA (2021) Advanced oxidation processes: photo-electro-Fenton remediation process for wastewater contaminated by organic azo dyes. Int J Environ Anal Chem 101:2947–2962. https://doi.org/10.1080/03067319.2020.1711892

Larbi KH, Habelhames F, Lakhdari M, et al (2021) A comparative study of a direct and pulse electrode-position method of $TiO_2$ films and its effect on photo-electrocatalytic degradation of methyl orange dye. Optoelectron Lett 17:334–341. https://doi.org/10.1007/S11801-021-0193-4/METRICS

Lian Z, Tao Y, Liu Y, et al (2020) Efficient Self-Driving Photoelectrocatalytic Reactor for Synergistic Water Purification and $H_2$ Evolution. ACS Appl Mater Interfaces 12:44731–44742. https://doi.org/10.1021/ACSAMI.0C12828

Liu CF, Huang CP, Hu CC, Huang C (2019a) A dual $TiO_2$/Ti-stainless steel anode for the degradation of orange G in a coupling photoelectrochemical and photo-electro-Fenton system. Sci Total Environ 659:221–229. https://doi.org/10.1016/J.SCITOTENV.2018.12.224

Liu YH, Kuo YS, Liu WC, Chou WL (2021) Photoelectrocatalytic activity of perovskite YFeO3/carbon fiber composite electrode under visible light irradiation for organic wastewater treatment. J Taiwan Inst Chem Eng 128:227–236. https://doi.org/10.1016/J.JTICE.2021.08.029

Liu Z, Song Y, Wang Q, et al (2019b) Solvothermal fabrication and construction of highly photoelectrocatalytic $TiO_2$ NTs/$Bi_2MoO_6$ heterojunction based on titanium mesh. J Colloid

Interface Sci 556:92–101. https://doi.org/10.1016/J.JCIS.2019.08.038

Long X, Pan Q, Wang C, et al (2017) Microbial fuel cell-photoelectrocatalytic cell combined system for the removal of azo dye wastewater. Bioresour Technol 244:182–191. https://doi.org/10.1016/J.BIORTECH.2017.07.088

Long X, Wang H, Wang C, et al (2019) Enhancement of azo dye degradation and power generation in a photoelectrocatalytic microbial fuel cell by simple cathodic reduction on titania nanotube arrays electrode. J Power Sources 415:145–153. https://doi.org/10.1016/J.JPOWSOUR.2019.01.069

Lu Q, Yu Y, Ma Q, et al (2016) 2D Transition-Metal-Dichalcogenide-Nanosheet-Based Composites for Photocatalytic and Electrocatalytic Hydrogen Evolution Reactions. Adv Mater 28:1917–1933. https://doi.org/10.1002/adma.201503270

Ma D, Yi H, Lai C, et al (2021) Critical review of advanced oxidation processes in organic wastewater treatment. Chemosphere 275:130104. https://doi.org/10.1016/J.CHEMOSPHERE.2021.130104

Ma M, Huang Y, Liu J, et al (2020) Engineering the photoelectrochemical behaviors of ZnO for efficient solar water splitting. J Semicond 41:. https://doi.org/10.1088/1674-4926/41/9/091702

Macedo LC, Zaia DAM, Moore GJ, de Santana H (2007) Degradation of leather dye on $TiO_2$: A study of applied experimental parameters on photoelectrocatalysis. J Photochem Photobiol A Chem 185:86–93. https://doi.org/10.1016/J.JPHOTOCHEM.2006.05.016

Mahmoudi N, Farhadian M, Solaimany Nazar AR, et al (2022) Investigation and optimization of the performance of sono-photo-electro-Fenton process for removal of Acid Black 172 and Disperse Blue 56 from polluted water: comparison of the degradation activity with electro-Fenton-based processes. Int J Environ Sci Technol 19:1671–1682. https://doi.org/10.1007/S13762-021-03296-0/FIGURES/6

Márquez AA, Coreño O, Nava JL (2022a) A hybrid process combining electrocoagulation and active chlorine-based photoelectro-Fenton-like methods during the removal of Acid Blue 29 dye. J Electroanal Chem 922:116732. https://doi.org/10.1016/J.JELECHEM.2022.116732

Márquez AA, Coreño O, Nava JL (2022b) An innovative process combining electrocoagulation and photoelectro-Fenton-like methods during the abatement of Acid Blue 113 dye. Process Saf Environ Prot 163:475–486. https://doi.org/10.1016/J.PSEP.2022.05.061

Márquez AA, Sirés I, Brillas E, Nava JL (2020) Mineralization of Methyl Orange azo dye by processes based on H2O2 electrogeneration at a 3D-like air-diffusion cathode. Chemosphere 259:127466. https://doi.org/10.1016/J.CHEMOSPHERE.2020.127466

Martins AS, Lachgar A, Boldrin Zanoni MV (2020) Sandwich Nylon/stainless-steel/$WO_3$

membrane for the photoelectrocatalytic removal of Reactive Red 120 dye applied in a flow reactor. Sep Purif Technol 237:116338. https://doi.org/10.1016/J.SEPPUR.2019.116338

McMichael S, Fernández-Ibáñez P, Byrne JA (2021) A Review of Photoelectrocatalytic Reactors for Water and Wastewater Treatment. Water 2021, Vol 13, Page 1198 13:1198. https://doi.org/10.3390/W13091198

Medrano-Rodríguez F, Picos-Benítez A, Brillas E, et al (2020) Electrochemical advanced oxidation discoloration and removal of three brown diazo dyes used in the tannery industry. J Electroanal Chem 873:114360. https://doi.org/10.1016/J.JELECHEM.2020.114360

Meng HS, Liu Y, Liu PX, et al (2021) Development of a three-dimensional photoelectrocatalytic reactor packed with granular sludge carbon photoelectrocatalyst for efficient wastewater treatment. Sep Purif Technol 277:119642. https://doi.org/10.1016/J.SEPPUR.2021.119642

Meng X, Zhang Z, Li X (2015) Synergetic photoelectrocatalytic reactors for environmental remediation: A review. J Photochem Photobiol C Photochem Rev 24:83–101. https://doi.org/10.1016/J.JPHOTOCHEMREV.2015.07.003

Moradi M, Ghanbari F, Minaee Tabrizi E (2015) Removal of acid yellow 36 using Box–Behnken designed photoelectro-Fenton: a study on removal mechanisms. Toxicol Environ Chem 97:700–709. https://doi.org/10.1080/02772248.2015.1060975

Moreira FC, Garcia-Segura S, Vilar VJP, et al (2013) Decolorization and mineralization of Sunset Yellow FCF azo dye by anodic oxidation, electro-Fenton, UVA photoelectro-Fenton and solar photoelectro-Fenton processes. Appl Catal B Environ 142–143:877–890. https://doi.org/10.1016/J.APCATB.2013.03.023

Mousset E, Dionysiou DD (2020) Photoelectrochemical reactors for treatment of water and wastewater: a review. Environ Chem Lett 2020 184 18:1301–1318. https://doi.org/10.1007/S10311-020-01014-9

Mumjitha M, Raj V (2015) Electrochemical synthesis, structural features and photoelectrocatalytic activity of $TiO_2$–$SiO_2$ ceramic coatings on dye degradation. Mater Sci Eng B 198:62–73. https://doi.org/10.1016/J.MSEB.2015.03.020

Murrieta MF, Sirés I, Brillas E, Nava JL (2020) Mineralization of Acid Red 1 azo dye by solar photoelectro-Fenton-like process using electrogenerated HClO and photoregenerated Fe(II). Chemosphere 246:125697. https://doi.org/10.1016/J.CHEMOSPHERE.2019.125697

Nabizadeh Chianeh F, Basiri Parsa J (2015) Degradation of azo dye in aqueous solution using Ti anode coated with MWCNTs-$TiO_2$. J Iran Chem Soc 12:175–182. https://doi.org/10.1007/S13738-014-0471-1

Nidheesh P V., Zhou M, Oturan MA (2018) An overview on the removal of synthetic dyes from water by electrochemical advanced oxidation processes. Chemosphere 197:210–227.

https://doi.org/10.1016/J.CHEMOSPHERE.2017.12.195

Nkwachukwu O V., Muzenda C, Ojo BO, et al (2021) Photoelectrochemical degradation of organic pollutants on a $La^{3+}$ doped $BiFeO_3$ perovskite. Catalysts 11:1069. https://doi.org/10.3390/CATAL11091069/S1

Nurdin M, Muzakkar MZ, Maulidiyah M, et al (2022) Highly active visible-light-driven photo-electrocatalytic process in $TiO_2$/Ti electrode by Te doping. J Appl Electrochem 1:1–8. https://doi.org/10.1007/S10800-022-01771-1/FIGURES/6

Nurdin M, Nuhung S, Musdalifah A, et al (2021) Cu-$TiO_2$ doped Ti thin-layer photoelectrode for visible-light induced photoelectrocatalytic activities: degradation of methylene orange. J Phys Conf Ser 1899:012042. https://doi.org/10.1088/1742-6596/1899/1/012042

Nwahara N, Adeniyi O, Mashazi P, Nyokong T (2021) Visible light responsive $TiO_2$ - graphene oxide nanosheets - Zn phthalocyanine ternary heterojunction assisted photoelectrocatalytic degradation of Orange G. J Photochem Photobiol A Chem 414:113291. https://doi.org/10.1016/J.JPHOTOCHEM.2021.113291

Ochiai T, Fujishima A (2012) Photoelectrochemical properties of $TiO_2$ photocatalyst and its applications for environmental purification. J Photochem Photobiol C Photochem Rev 13:247–262. https://doi.org/10.1016/J.JPHOTOCHEMREV.2012.07.001

Of THEJ, Shankar K, Basham JI, et al (2009) Recent Advances in the Use of $TiO_2$ Nanotube and Nanowire Arrays for Oxidative photoelectrochemistry. J Phys Chem C 113:6327–6359. https://doi.org/10.1021/jp809385x

Olya ME, Pirkarami A, Soleimani M, Bahmaei M (2013) Photoelectrocatalytic degradation of acid dye using Ni–$TiO_2$ with the energy supplied by solar cell: Mechanism and economical studies. J Environ Manage 121:210–219. https://doi.org/10.1016/J.JENVMAN.2013.01.041

Orimolade BO, Arotiba OA (2019) An Exfoliated Graphite-Bismuth Vanadate Composite Photoanode for the Photoelectrochemical Degradation of Acid Orange 7 Dye. Electrocatalysis 10:429–435. https://doi.org/10.1007/S12678-019-00534-5/FIGURES/6

Orudzhev F, Ramazanov S, Sobola D, et al (2020) Atomic layer deposition of mixed-layered aurivillius phase on $TiO_2$ nanotubes: Synthesis, characterization and photoelectrocatalytic properties. Nanomaterials 10:1–16. https://doi.org/10.3390/nano10112183

Orudzhev FF, Ramazanov SM, Isaev AB, et al (2019) Self-organization of layered perovskites on $TiO_2$ nanotubes surface by atomic layer deposition. Mater Today Proc 36:364–367. https://doi.org/10.1016/j.matpr.2020.04.153

Oturan MA (2014) Electrochemical advanced oxidation technologies for removal of organic pollutants from water. Environ Sci Pollut Res 21:8333–8335. https://doi.org/10.1007/S11356-014-2841-8/METRICS

Panizza M, Cerisola G (2009) Direct And Mediated Anodic Oxidation of Organic Pollutants. Chem Rev 109:6541–6569. https://doi.org/10.1021/CR9001319

Paz EC, Aveiro LR, Pinheiro VS, et al (2018) Evaluation of $H_2O_2$ electrogeneration and decolorization of Orange II azo dye using tungsten oxide nanoparticle-modified carbon. Appl Catal B Environ 232:436–445. https://doi.org/10.1016/J.APCATB.2018.03.082

Paz EC, Pinheiro VS, Joca JFS, et al (2020) Removal of Orange II (OII) dye by simulated solar photoelectro-Fenton and stability of $WO_{2.72}$/Vulcan XC72 gas diffusion electrode. Chemosphere 239:124670. https://doi.org/10.1016/J.CHEMOSPHERE.2019.124670

Peleyeju MG, Arotiba OA (2018) Recent trend in visible-light photoelectrocatalytic systems for degradation of organic contaminants in water/wastewater. Environ Sci Water Res Technol 4:1389–1411. https://doi.org/10.1039/C8EW00276B

Peralta-Hernández JM, Méndez-Tovar M, Guerra-Sánchez R, et al (2012) A Brief Review on Environmental Application of Boron Doped Diamond Electrodes as a New Way for Electrochemical Incineration of Synthetic Dyes. Int J Electrochem 2012:1–18. https://doi.org/10.1155/2012/154316

Pereira GF, El-Ghenymy A, Thiam A, et al (2016) Effective removal of Orange-G azo dye from water by electro-Fenton and photoelectro-Fenton processes using a boron-doped diamond anode. Sep Purif Technol 160:145–151. https://doi.org/10.1016/J.SEPPUR.2016.01.029

Pinheiro ACN, Bernardino TS, Junior FEB, et al (2020) Enhanced electrodegradation of the Sunset Yellow dye in acid media by heterogeneous Photoelectro-Fenton process using $Fe_3O_4$ nanoparticles as a catalyst. J Environ Chem Eng 8:103621. https://doi.org/10.1016/J.JECE.2019.103621

Qiu L, Wang Q, Liu Z, et al (2018) Preparation of 3D $TiO_2$ nanotube arrays photoelectrode on Ti mesh for photoelectric conversion and photoelectrocatalytic removal of pollutant. Sep Purif Technol 207:206–212. https://doi.org/10.1016/J.SEPPUR.2018.06.050

Qu Y, Duan X (2013) Progress, challenge and perspective of heterogeneous photocatalysts. Chem Soc Rev 42:2568–2580. https://doi.org/10.1039/c2cs35355e

Rajput H, Kwon EE, Younis SA, et al (2021) Photoelectrocatalysis as a high-efficiency platform for pulping wastewater treatment and energy production. Chem Eng J 412:128612. https://doi.org/10.1016/J.CEJ.2021.128612

Ramírez J, Godínez LA, Méndez M, et al (2010) Heterogeneous photo-electro-Fenton process using different iron supporting materials. J Appl Electrochem 40:1729–1736. https://doi.org/10.1007/S10800-010-0157-Z

Rawat D, Mishra V, Sharma RS (2016) Detoxification of azo dyes in the context of environmental processes. Chemosphere 155:591–605.

https://doi.org/10.1016/J.CHEMOSPHERE.2016.04.068

Robles I, Rodríguez-Valadez FJ, Castaño E, Godínez LA (2017) Study of the influence of the operational parameters on the photoelectro-Fenton performance of an industrial wastewater treatment prototype using Orange II as a model pollutant. Sustain Environ Res 27:24–31. https://doi.org/10.1016/J.SERJ.2016.08.004

Ruiz EJ, Arias C, Brillas E, et al (2011a) Mineralization of Acid Yellow 36 azo dye by electro-Fenton and solar photoelectro-Fenton processes with a boron-doped diamond anode. Chemosphere 82:495–501. https://doi.org/10.1016/J.CHEMOSPHERE.2010.11.013

Ruiz EJ, Hernández-Ramírez A, Peralta-Hernández JM, et al (2011b) Application of solar photoelectro-Fenton technology to azo dyes mineralization: Effect of current density, Fe2+ and dye concentrations. Chem Eng J 171:385–392. https://doi.org/10.1016/J.CEJ.2011.03.004

Salazar R, Gallardo-Arriaza J, Vidal J, et al (2019a) Treatment of industrial textile wastewater by the solar photoelectro-Fenton process: Influence of solar radiation and applied current. Sol Energy 190:82–91. https://doi.org/10.1016/j.solener.2019.07.072

Salazar R, Gallardo-Arriaza J, Vidal J, et al (2019b) Treatment of industrial textile wastewater by the solar photoelectro-Fenton process: Influence of solar radiation and applied current. Sol Energy 190:82–91. https://doi.org/10.1016/J.SOLENER.2019.07.072

Salazar R, Ureta-Zañartu MS (2012) Degradation of acid violet 7 and reactive black 5 in water by electro-fenton and photo electro-fenton by. J Chil Chem Soc 57:999–1003. https://doi.org/10.4067/S0717-97072012000100010

Sboui M, Niu W, Li D, et al (2022) Fabrication of electrically conductive $TiO_2$/PANI/PVDF composite membranes for simultaneous photoelectrocatalysis and microfiltration of azo dye from wastewater. Appl Catal A Gen 644:118837. https://doi.org/10.1016/J.APCATA.2022.118837

Sboui M, Niu W, Lu G, et al (2023) Electrically conductive $TiO_2$/CB/PVDF membranes for synchronous cross-flow filtration and solar photoelectrocatalysis. Chemosphere 310:136753. https://doi.org/10.1016/J.CHEMOSPHERE.2022.136753

Shabanov NS, Asvarov AS, Chiolerio A, et al (2017) Peroxy-Titanium Complex-based inks for low temperature compliant anatase thin films. J Colloid Interface Sci 498:306–312. https://doi.org/10.1016/j.jcis.2017.03.075

Shinde PS, Patil PS, Bhosale PN, et al (2009) UVA and solar light assisted photoelectrocatalytic degradation of AO7 dye in water using spray deposited $TiO_2$ thin films. Appl Catal B Environ 89:288–294. https://doi.org/10.1016/J.APCATB.2009.02.025

Sirés I, Brillas E, Oturan MA, et al (2014a) Electrochemical advanced oxidation processes:

1307 Today and tomorrow. A review. Environ Sci Pollut Res 21:8336–8367.
1308 https://doi.org/10.1007/s11356-014-2783-1
1309 Sirés I, Brillas E, Oturan MA, et al (2014b) Electrochemical advanced oxidation processes:
1310 Today and tomorrow. A review. Environ Sci Pollut Res 21:8336–8367.
1311 https://doi.org/10.1007/S11356-014-2783-1/TABLES/4
1312 Solano AMS, Garcia-Segura S, Martínez-Huitle CA, Brillas E (2015) Degradation of acidic
1313 aqueous solutions of the diazo dye Congo Red by photo-assisted electrochemical processes
1314 based on Fenton's reaction chemistry. Appl Catal B Environ 168–169:559–571.
1315 https://doi.org/10.1016/J.APCATB.2015.01.019
1316 Subba Rao AN, Venkatarangaiah VT, Nagarajappa GB, et al (2017) Enhancement in the photo-
1317 electrocatalytic activity of $SnO_2$-$Sb_2O_4$ mixed metal oxide anode by nano-WO3
1318 modification: Application to trypan blue dye degradation. J Environ Chem Eng 5:4969–
1319 4979. https://doi.org/10.1016/J.JECE.2017.09.033
1320 Suhadolnik L, Pohar A, Novak U, et al (2019) Continuous photocatalytic, electrocatalytic and
1321 photo-electrocatalytic degradation of a reactive textile dye for wastewater-treatment
1322 processes: Batch, microreactor and scaled-up operation. J Ind Eng Chem 72:178–188.
1323 https://doi.org/10.1016/J.JIEC.2018.12.017
1324 Tang W, Chen X, Xia J, et al (2014) Preparation of an Fe-doped visible-light-response TiO2 film
1325 electrode and its photoelectrocatalytic activity. Mater Sci Eng B 187:39–45.
1326 https://doi.org/10.1016/J.MSEB.2014.04.011
1327 Tantis I, Stathatos E, Mantzavinos D, Lianos P (2015) Photoelectrocatalytic degradation of
1328 potential water pollutants in the presence of NaCl using nanocrystalline titania films. J
1329 Chem Technol Biotechnol 90:1338–1344. https://doi.org/10.1002/JCTB.4549
1330 Thabet M, El-Zomrawy AA (2016) Degradation of acid red 17 dye with ammonium persulphate
1331 in acidic solution using photoelectrocatalytic methods. Arab J Chem 9:S204–S208.
1332 https://doi.org/10.1016/J.ARABJC.2011.03.001
1333 Thiam A, Sirés I, Brillas E (2015a) Treatment of a mixture of food color additives (E122, E124
1334 and E129) in different water matrices by UVA and solar photoelectro-Fenton. Water Res
1335 81:178–187. https://doi.org/10.1016/J.WATRES.2015.05.057
1336 Thiam A, Sirés I, Centellas F, et al (2015b) Decolorization and mineralization of Allura Red AC
1337 azo dye by solar photoelectro-Fenton: Identification of intermediates. Chemosphere 136:1–
1338 8. https://doi.org/10.1016/J.CHEMOSPHERE.2015.03.047
1339 Thongthep P, Moonmangmee S, Ponchio C (2021) Solar/photoelectrocatalytic cell development
1340 for $H_2$ production and simultaneous organic dye degradation. Mater Sci Semicond Process
1341 124:105597. https://doi.org/10.1016/J.MSSP.2020.105597

Thor SH, Ho LN, Ong SA, et al (2021) Advanced oxidation treatment of amaranth dye synchronized with electricity generation using carbon-based cathodes in a sustainable photocatalytic fuel cell integrated electro-fenton system. J Environ Chem Eng 9:106439. https://doi.org/10.1016/J.JECE.2021.106439

Tian H, Zhou X, Zhang Y, et al (2021) High photoelectrocatalytic activity of selenium (Se) doped $TiO_2$/Ti electrode for degradation of reactive orange 84. J Phys Conf Ser 1899:012046. https://doi.org/10.1088/1742-6596/1899/1/012046

Titchou FE, Zazou H, Afanga H, et al (2022) Comparative study of the removal of direct red 23 by anodic oxidation, electro-Fenton, photo-anodic oxidation and photoelectro-Fenton in chloride and sulfate media. Environ Res 204:112353. https://doi.org/10.1016/J.ENVRES.2021.112353

Turolla A, Bestetti M, Antonelli M (2018) Optimization of heterogeneous photoelectrocatalysis on nanotubular $TiO_2$ electrodes: Reactor configuration and kinetic modelling. Chem Eng Sci 182:171–179. https://doi.org/10.1016/J.CES.2018.02.041

Vasudevan S, Oturan MA (2014) Electrochemistry: As cause and cure in water pollution-an overview. Environ Chem Lett 12:97–108. https://doi.org/10.1007/S10311-013-0434-2

Wang A, Qu J, Liu H, Ru J (2008) Mineralization of an azo dye Acid Red 14 by photoelectro-Fenton process using an activated carbon fiber cathode. Appl Catal B Environ 84:393–399. https://doi.org/10.1016/J.APCATB.2008.04.016

Wang P, Ao Y, Wang C, et al (2012) Enhanced photoelectrocatalytic activity for dye degradation by graphene–titania composite film electrodes. J Hazard Mater 223–224:79–83. https://doi.org/10.1016/J.JHAZMAT.2012.04.050

Wang P, Cao M, Ao Y, et al (2011) Investigation on Ce-doped $TiO_2$-coated BDD composite electrode with high photoelectrocatalytic activity under visible light irradiation. Electrochem commun 13:1423–1426. https://doi.org/10.1016/J.ELECOM.2011.09.009

Wang R, Cao J, Song J, et al (2022) Application of boron doped diamond for electro-Fenton and photoelectro-Fenton decolorization of azo dye from dye- containing wastewater: Acid Red 1. Int J Electrochem Sci 17:220249–220251. https://doi.org/10.20964/2022.02.45

Wei J, Liang P, Huang X (2011) Recent progress in electrodes for microbial fuel cells. Bioresour Technol 102:9335–9344. https://doi.org/10.1016/J.BIORTECH.2011.07.019

Xing L, Jia J, Wang Y, Dong S (2013) Lanthanide-doped $TiO_2$ nanoparticles–modified electrode for photoelectrocatalytic degradation of dye. Environ Prog Sustain Energy 32:302–306. https://doi.org/10.1002/EP.11629

Xu Y, Zhong D, Jia J, et al (2013) Dual slant-placed electrodes thin-film photocatalytic reactor: Enhanced dye degradation efficiency by self-generated electric field. Chem Eng J 225:138–

143. https://doi.org/10.1016/J.CEJ.2013.03.085

Ye S, Chen Y, Yao X, Zhang J (2021) Simultaneous removal of organic pollutants and heavy metals in wastewater by photoelectrocatalysis: A review. Chemosphere 273:128503. https://doi.org/10.1016/J.CHEMOSPHERE.2020.128503

Yuan CS, Ie IR, Zheng JR, et al (2021) A Review of Electrical Assisted Photocatalytic Technologies for the Treatment of Multi-Phase Pollutants. Catal 2021, Vol 11, Page 1332 11:1332. https://doi.org/10.3390/CATAL11111332

Yusuf TL, Orimolade BO, Masekela D, et al (2022) The application of photoelectrocatalysis in the degradation of rhodamine B in aqueous solutions: a review. RSC Adv 12:26176–26191. https://doi.org/10.1039/D2RA04236C

Zarei E, Ojani R (2016) Fundamentals and some applications of photoelectrocatalysis and effective factors on its efficiency: a review. J Solid State Electrochem 2016 212 21:305–336. https://doi.org/10.1007/S10008-016-3385-2

Zarei M, Khataee AR, Ordikhani-Seyedlar R, Fathinia M (2010) Photoelectro-Fenton combined with photocatalytic process for degradation of an azo dye using supported $TiO_2$ nanoparticles and carbon nanotube cathode: Neural network modeling. Electrochim Acta 55:7259–7265. https://doi.org/10.1016/J.ELECTACTA.2010.07.050

Zeng L, He Z, Luo Y, et al (2021) A Simple g-$C_3N_4$/TNTs Heterojunction for Improving the Photoelectrocatalytic Degradation of Methyl Orange. J Electrochem Soc 168:116520. https://doi.org/10.1149/1945-7111/AC3ABC

Zhang H, Chen G, Bahnemann DW (2009) Photoelectrocatalytic materials for environmental applications. J Mater Chem 19:5089. https://doi.org/10.1039/b821991e

Zhang H, Li Y, Zhong X, Ran X (2011) Application of experimental design methodology to the decolorization of Orange II using low iron concentration of photoelectro-Fenton process. Water Sci Technol 63:1373–1380. https://doi.org/10.2166/WST.2011.192

Zhang M, Yuan S, Wang Z, et al (2013) Photoelectrocatalytic properties of $Cu^{2+}$-doped $TiO_2$ film under visible light. Appl Catal B Environ 134–135:185–192. https://doi.org/10.1016/J.APCATB.2013.01.024

Zhang X, Yu W, Guo Y, et al (2023) Recent advances in photoelectrocatalytic advanced oxidation processes: From mechanism understanding to catalyst design and actual applications. Chem Eng J 455:140801. https://doi.org/10.1016/J.CEJ.2022.140801

Zhang Y, Xiong X, Han Y, et al (2012) Photoelectrocatalytic degradation of recalcitrant organic pollutants using $TiO_2$ film electrodes: An overview. Chemosphere 88:145–154. https://doi.org/10.1016/J.CHEMOSPHERE.2012.03.020

Zhang Z, Yuan Y, Liang L, et al (2008) Preparation and photoelectrocatalytic activity of ZnO

1412 nanorods embedded in highly ordered $TiO_2$ nanotube arrays electrode for azo dye
1413 degradation. J Hazard Mater 158:517–522.
1414 https://doi.org/10.1016/J.JHAZMAT.2008.01.118
1415 Zhao Q, Li X, Wang N, et al (2009) Facile fabrication, characterization, and enhanced
1416 photoelectrocatalytic degradation performance of highly oriented $TiO_2$ nanotube arrays. J
1417 Nanoparticle Res 11:2153–2162. https://doi.org/10.1007/S11051-009-9685-Z/FIGURES/11
1418 Zheng Q, Lee C (2014) Visible light photoelectrocatalytic degradation of methyl orange using
1419 anodized nanoporous $WO_3$. Electrochim Acta 115:140–145.
1420 https://doi.org/10.1016/J.ELECTACTA.2013.10.148
1421
1422
1423